AMERICAN JOURNAL OF PHYSICAL ANTHROPOLOGY 102:203–232 (1997)

In Vivo Bone Strain Patterns in the Zygomatic Arch of Macaques and the Significance of These Patterns for Functional Interpretations of Craniofacial Form

WILLIAM L. HYLANDER* AND KIRK R. JOHNSON
Duke University Medical Center, Department of Biological Anthropology and Anatomy, Durham, North Carolina 27710

KEY WORDS zygomatic arch; in vivo bone strain; functional morphology; jaw muscle force; mastication; primates

ABSTRACT It has been proposed that the mammalian facial skeleton is optimized for countering or dissipating masticatory stress. As optimized load-bearing structures by definition exhibit maximum strength with a minimum amount of material, this hypothesis predicts that during chewing and biting there should be relatively high and near uniform amounts of strain throughout the facial skeleton. If levels of strain in certain areas of the facial skeleton are relatively low during these behaviors, this indicates that the amount of bone mass in these areas could be significantly reduced without resulting in the danger of structural failure due to repeated masticatory loads. Furthermore, and by definition, this indicates that these areas are not optimized for countering masticatory stress, and instead their overall morphology and concentration of bone mass has most likely been selected or influenced mainly by factors unrelated to the dissipation or countering of chewing and biting forces.

An analysis of in vivo bone strain along the lateral aspect of the zygomatic arch of macaques indicates the clear absence of a high and near uniform strain environment throughout its extent. Instead, there is a steep strain gradient along the zygomatic arch, with the highest strains along its anterior portion, intermediate strains along its middle portion, and the lowest strains along its posterior portion. These data, in combination with earlier published data (Hylander et al., 1991), indicate that levels of functional strains during chewing and biting are highly variable from one region of the face to the next, and therefore it is unlikely that all facial bones are especially designed so as to minimize bone tissue and maximize strength for countering masticatory loads. Thus, the functional significance of the morphology of certain facial bones need not necessarily bear any important or special relationship to routine and habitual cyclical mechanical loads associated with chewing or biting. Furthermore, the presence of these steep strain gradients within the facial skeleton suggests that the amount of bone mass in the low-strain areas may be largely determined by factors unrelated to processes frequently referred to as "functional adaptation," or conversely, that the "optimal strain environment" of bone varies enormously throughout the facial skeleton (cf., Rubin et al., 1994).

Contract grant Sponsor NIH (Merit Award); Contract grant number DE04531; Contract grant sponsor NSF; Contract grant number SBR-9420764.

*Correspondence to: Professor William L. Hylander, Department of Biological Anthropology and Anatomy, Duke University Medical School, Box 3170, Durham, NC 27710.

Received 7 September 1995; Accepted 3 November 1996.

Based solely on anatomical considerations, it is likely that the zygomatic arch is bent in both the parasagittal and transverse planes and twisted about its long axis. Due to constraints on rosette position, the strain data are incapable of determining if one or more of these loading conditions predominate. Instead, the strain data simply provide limited support for the possible presence of all of these loading regimes. Finally, as the masseter muscle is concentrated along the anterior portion of the zygomatic arch and as the arch has fixed ends, the largest shearing forces and the largest bending and twisting moments are located along its anterior portion. This in turn explains why the largest strains are found along the anterior portion of the zygomatic arch. Am. J. Phys. Anthropol. 102:203–232, 1997

It has been proposed that the mammalian appendicular skeleton is optimized for load-bearing purposes (e.g., Roux, 1881; Koch, 1917; Weinman and Sicher, 1955; Kummer, 1972; Lanyon, 1973; Pauwels, 1980; Rubin, 1984; Frost, 1986; Kimmel, 1993; Rubin et al., 1994), i.e., the appendicular skeleton exhibits maximum strength with a minimum amount of bony material. Similarly, it is commonly thought (either implicitly or explicitly), as expressed by DuBrul (1988: 55), that the facial skeleton consists of "an optimal force-resisting framework for masticatory stress" (also cf. Seipel, 1948; Weinman and Sicher, 1955; Scott, 1967; Hylander, 1979a, 1985; Greaves, 1985; Russell, 1985; Preuschoft et al., 1986; Demes, 1987; Roberts et al., 1992; Biknevicius and Ruff, 1992).

As optimized load-bearing structures by definition exhibit maximum strength with a minimum amount of material, this hypothesis predicts that during chewing and biting there should be relatively high and near uniform amounts of strain throughout the facial skeleton. If levels of strain in certain areas of the facial skeleton are relatively low during these behaviors, this indicates that the amount of bone mass in these areas could be significantly reduced without resulting in the danger of structural failure due to repeated masticatory loads. Furthermore, and by definition, this also indicates that these low-strain areas are not optimized for countering masticatory stress, and instead their overall morphology and concentration of bone mass has most likely been selected or influenced mainly by factors unrelated to the dissipation or countering of chewing and biting forces (cf. Hylander et al., 1991).

A recent analysis of in vivo facial bone strain in macaques and baboons indicates the clear absence of a high and near uniform strain environment throughout the upper, middle and lower portions of the facial skeleton during mastication and incision (Hylander et al., 1991). For example, in adult macaques the mandible experiences 20 times more strain than does the rostral interorbital region. In general, it was found that the relatively high-strain areas of the face are located along the lateral aspect of the posterior mandibular corpus, the facial aspect of the anterior root of the zygoma, and the anterior portion of the zygomatic arch. In contrast, the low-strain areas are located along the dorsal orbital, and dorsal and rostral interorbital regions. More recently, preliminary data suggest the presence of a strain gradient along the lateral aspect of the zygomatic arch, with the highest strains along its anterior portion, intermediate strains along its middle portion, and the lowest strains during its posterior portion (Hylander and Johnson, 1992).

As levels of functional strains during chewing and biting are highly variable from one region of the face to the next, it appears unlikely that all facial bones are especially designed so as to minimize bone tissue and maximize strength for countering masticatory loads. If true, this presents major problems for those studies that have argued that the functional significance of the morphology of the upper portions of the face is related to countering internal stresses associated with chewing and biting (cf. Wolpoff, 1980; Oyen et al., 1979; Russell, 1985; Rak, 1983, 1986; Demes, 1987). As an alternative

explanation, perhaps some portions of the primate skull are designed so as to counter or dissipate relatively infrequent unintentional traumatic loads (Tappen, 1978; Hylander et al., 1991; Hylander and Ravosa, 1992). Moreover, perhaps the functional significance of certain portions of the skull are altogether unrelated to countering mechanical forces, and instead are due to spatial factors, i.e., the position of the face relative to the braincase (Moss and Young, 1960; Ravosa, 1988, 1991), or are simply secondary sex characters (Lanyon and Rubin, 1985). Finally, the presence of steep strain gradients within the facial skeleton suggests that the amount of bone mass in the low-strain areas may be largely determined by factors unrelated to processes frequently referred to as "functional adaptation" (cf. Goodship et al., 1979; Rubin, 1984; Lanyon and Rubin, 1985), or conversely, that the so-called "optimal strain environment" of bone varies enormously throughout the facial skeleton (cf. Lanyon et al., 1982; Rubin et al., 1994; Fig. 1).

The purpose of this study is to analyze in vivo bone strain patterns along the zygomatic arch in *Macaca fascicularis*, in part so as to confirm the possible presence of the antero-posterior strain gradient within this region. Thus, this study provides an additional test of the hypothesis that the facial skeleton is an optimal force-resisting framework for countering masticatory stress (Du Brul, 1988), although in this instance the morphological areas to be analyzed are immediately adjacent to one another and functionally are closely related to the masticatory apparatus. Moreover, as levels of functional strain[1] are thought to have a profound effect on the development of bone, a confirmation of a steep strain gradient and a detailed characterization of in vivo strain along the zygomatic arch provides an opportunity to test various hypotheses regarding the relationship between bone strain magnitude and bony architecture (e.g., Lanyon, 1991), in addition to modeling and remodeling events of bone (cf. Carter, 1984; Frost, 1986; Martin and Burr, 1989; Bouvier and Hylander, 1994, 1996, 1997). Furthermore, an analysis of in vivo bone strain from the zygomatic arch also provides insights as to how this region is loaded, which in turn may contribute to a better functional understanding of the morphological diversity of the zygomatic arch among primates. Although our study was not specifically designed to determine how the zygomatic arch is loaded, and/or twisted, our data play a limited role in evaluating various loading regimes.

Although preliminary data on strain gradients within the zygomatic arch of macaques have been presented elsewhere (Hylander and Johnson, 1992), the data in this earlier study were limited to principal strain magnitudes associated with only a small number of chewing cycles from just two separate experiments, and contained no information on the direction of these principal strains. In the present study we expand on the preliminary data by increasing the number of experiments and chewing cycles analyzed per experiment, and performing a much more detailed analysis of the patterns of strain, including the direction of the principal strains.

MATERIALS AND METHODS

Subjects

Three adult female (macaques 1, 2 and 5) and two subadult male (macaques 7 and 9) *Macaca fascicularis* served as subjects. All subjects had a Class I molar relationship, a full complement of posterior teeth in occlusion, and either an edge-to-edge incisor bite or an incisor overbite of no more than 1 mm.

Experiments

In all subjects except macaque 1, three rosette strain gages were bonded unilaterally along the lateral aspect of the zygomatic arch. One rosette was bonded immediately posterior and one immediately anterior to the zygomaticotemporal suture. The third rosette was bonded along the most anterior portion of the zygomatic arch (Fig. 2). All three zygomatic arch sites were easily identified during the bonding procedure, and therefore rosette position does not vary appreciably between experiments. In macaque

[1]Following Lanyon and Rubin (1985), functional strain refers to strains associated with routine behaviors such as chewing, running, flying, breathing, etc. Strains associated with various sorts of infrequent traumatic loads, such as a blow to the side of the head due to a fall from a tree, are not referred to as functional strains.

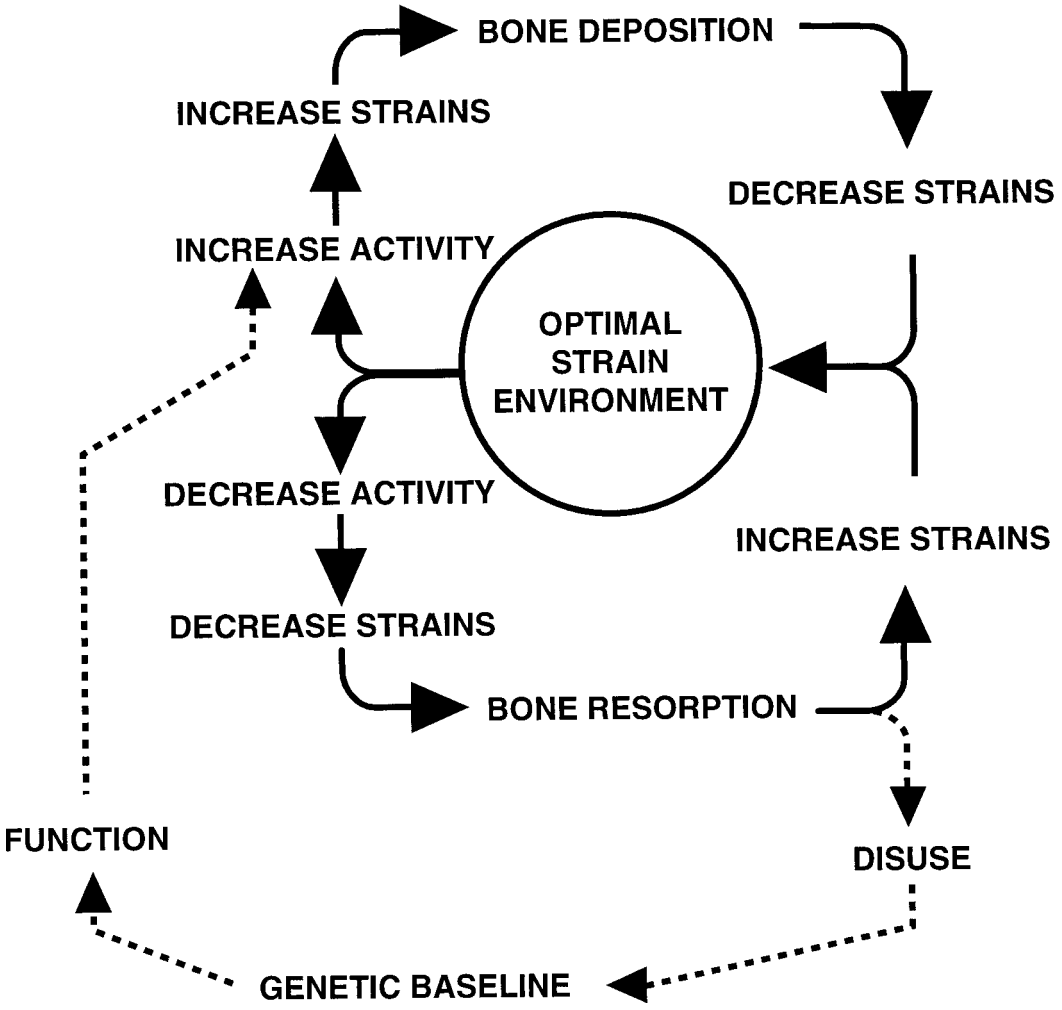

Fig. 1. The process of "functional adaptation" i.e., the effects of an increase or decrease in functional strains on bone mass so as to achieve an optimal strain environment (Rubin, 1984). Increased activity that causes functional strains to rise above the "optimal strain environment" stimulates bone deposition. This increases skeletal mass, which in turn decreases functional strains so that the altered strains now lie within the limits of the "optimal strain environment." Decreased activity that causes functional strains to fall below the "optimal strain environment" stimulates bone resorption. This decreases skeletal mass, which in turn increases functional strains so that the altered strains now lie within the limits of the "optimal strain environment." Complete disuse causes continued loss of bone mass until a "genetic baseline" equilibrium point has been reached. According to Rubin (1984) . . . . "Some skeletal organs (e.g., auditory ossicles, cranium) will develop fully without exposure to a dynamic environment, and probably represent this baseline" (legend for Fig. 1, p. S12). This figure is redrawn from Rubin (1984).

1, a single rosette was bonded unilaterally along the most anterior part of the left arch.

Rosette alignment for all experiments was determined from radiographs and/or directly during the bonding procedure. Rosette position was determined by measuring with sliding calipers the distance between the zygomaticotemporal suture and the center of each rosette. For all subjects, bone strain data were recorded as they incised and chewed various foods.

Rosette bonding procedure

The procedure and apparatus for bonding miniature 120-ohm stacked rosettes (SA-06-030WY-120, Micro-Measurements, Raleigh,

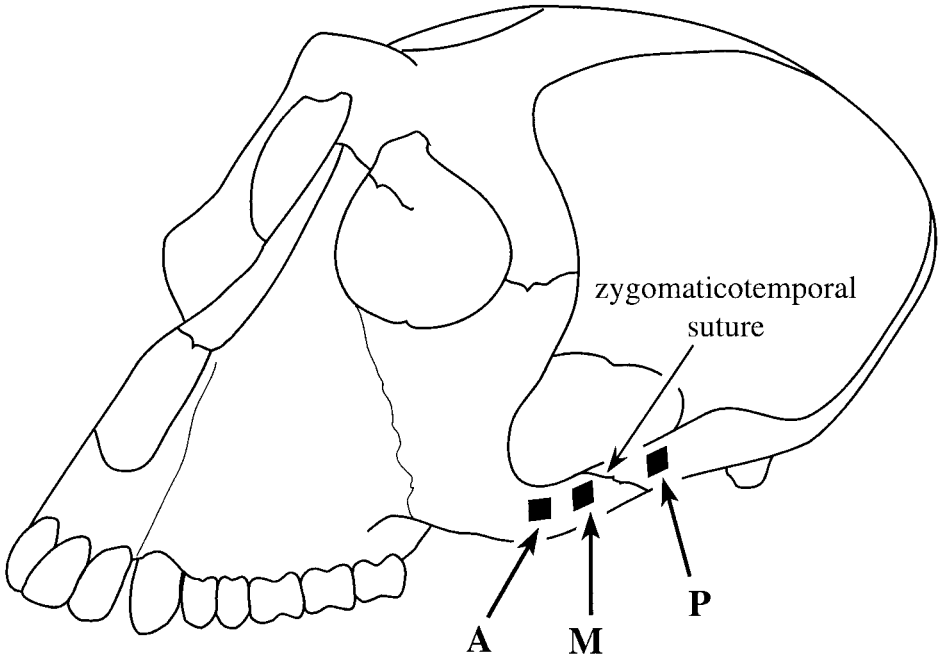

Fig. 2. The labeled arrows point to the location of the anterior (A), middle (M), and posterior (P) portions of the zygomatic arch.

NC) to cortical bone with a cyanoacrylate adhesive are described elsewhere (Hylander, 1984, 1986; Hylander and Johnson, 1989). These procedures were performed with the subjects heavily sedated with a combination of acepromazine and ketamine (Connolly and Quimby, 1978). Before bonding, the surgical site was infiltrated subcutaneously with a local anesthetic (lidocaine HCl) containing epinephrine (1:100,000) so as to provide anesthesia and adequate hemostasis. The masseter muscle and temporalis fascia were unaltered by our surgical procedures.

Recording procedure

Each of the strain-gage elements of each rosette formed one arm of a Wheatstone bridge. Bridge excitation for each element was 1 volt. The voltage output from each of the strain-gage elements was first conditioned and amplified (Vishay 2100 System, Vishay Instruments, Raleigh, NC) and then recorded at 15 inches per second with a 14-channel FM tape recorder (Bell and Howell CPR4020A, Datatape Division, Pasadena, CA). We also recorded on the voice track of the tape recorder whether the subject chewed on the left or right side. Details of the recording procedure are the same as described previously (Hylander et al., 1991).

Prior to recovery from sedation, the subject was placed in a restraining chair especially designed to permit normal head, neck, and jaw movements during mastication. Once the animal was fully alert, usually 5–6 hours later, it was fed pieces of monkey chow, apple skin, dried apricot, popcorn kernels, hard unripe pear, and prune seeds. These foods were chosen to elicit a wide range of masticatory forces.

Data analysis

Immediately before and after each sequence of mastication, the zero level of strain was determined as the monkey sat with its mandible at rest. The subject was fed various foods in an intermittent and random fashion and data were recorded until either sufficient data were obtained or the animal refused to eat any additional food. At the conclusion of the recording session, the animal was sedated and anesthetized, the ro-

settes were removed, the surgical incisions were resutured, antibiotics were administered, and the animal was returned to its cage. Recovery from the procedures and healing of the surgical incisions were uneventful in all subjects.

Strain analysis

All bone strain recordings of each chewing sequence were initially reproduced for visual examination by playing the raw strain data from the tape recorder into a six-channel chart recorder (Brush 260, Gould Inc., Cleveland, OH). Two complete chewing sequences of each food eaten were selected for analysis. One sequence consisted of chews on the left side and the other of chews on the right side. The raw strains of all chewing cycles for each selected sequence were played simultaneously from the FM tape recorder into a 16-channel analog-to-digital converter (Model NB-MIO-16H-9, 12-bit resolution, National Instruments Corporation, Austin, TX), and the digitized values were written to the hard disk of a microcomputer (Macintosh Quadra 800, Apple Computer, Inc., Cupertino, CA). Each channel was sampled and digitized at a rate of 500 Hertz (Hz) with a channel separation time of 0.125 milliseconds (ms). The digitized values were then read back into the microcomputer for subsequent processing and analysis using programs written in the LabVIEW 2 graphical programming system (National Instruments Corporation).

The digitized raw strain values were filtered at 40 Hz using a digital low-pass Butterworth filter. The magnitude of the maximum and minimum principal strains (ϵ_1 and ϵ_2) and maximum shear strains (γmax) were calculated in 2-ms intervals. For purposes of analysis, γmax was used as an indicator of peak strain (Hylander and Johnson, 1989). As ϵ_1 is a positive value (tension) and ϵ_2 is a negative value (compression) in our experiments, γmax is larger than either of the two principal strains because $\gamma\text{max} = \epsilon_1 - \epsilon_2$. The direction of ϵ_1 (the angle ϕ) was also calculated in 2-ms intervals. The angle ϕ was determined relative to the long axis of the zygomatic arch (Fig. 3). Descriptive statistics of ϵ_1, ϵ_2, γmax, ϵ_1/ϵ_2 and ϕ were calculated for peak strain, and for the 25%, 50% and 75% level of peak strain for both loading and unloading of each power stroke of mastication and incision.

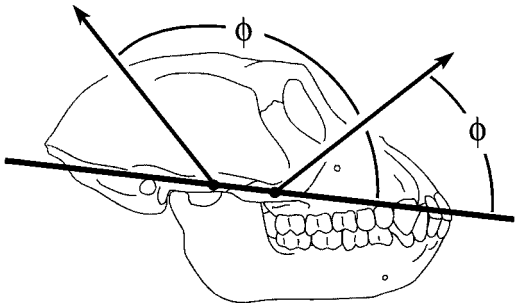

Fig. 3. This drawing indicates the construction of the angle ϕ along the rosette sites for the right zygomatic arch. In the interests of simplifying this figure, the middle rosette site for the zygomatic arch has not been included. The arrows indicate the direction of the maximum principal strain (ϵ_1).

RESULTS

Similar to our earlier studies, we encountered various behavioral problems during the recording procedures. For example, only macaques 1 and 9 vigorously incised into the various food items. Most notably, some subjects refused to eat certain foods. Moreover, when various foods were eaten, some subjects occasionally chewed on only one side. Fortunately all subjects readily chewed apple skin and at least one of the more mechanically resistant food items (i.e., monkey biscuit, popcorn kernels, prune seed, or hard unripe pear). Therefore, as in our earlier studies, we have presented strain data recorded during the chewing of a mechanically resistant food item, and also during the chewing of apple with skin. Data associated with the chewing of those foods that caused the largest strains are presented primarily because structural adaptations to counter masticatory stress are presumably in response to the more intense masticatory loading regimes. The presentation of zygomatic-arch strains recorded during the chewing of apple skin facilitates the comparison of these strains to strains recorded from other regions of the face during the chewing of apple skin (e.g., Hylander et al., 1991).

Strain magnitude

Figure 4 is a plot of time versus principal strain magnitudes (ϵ_1 and ϵ_2) recorded from

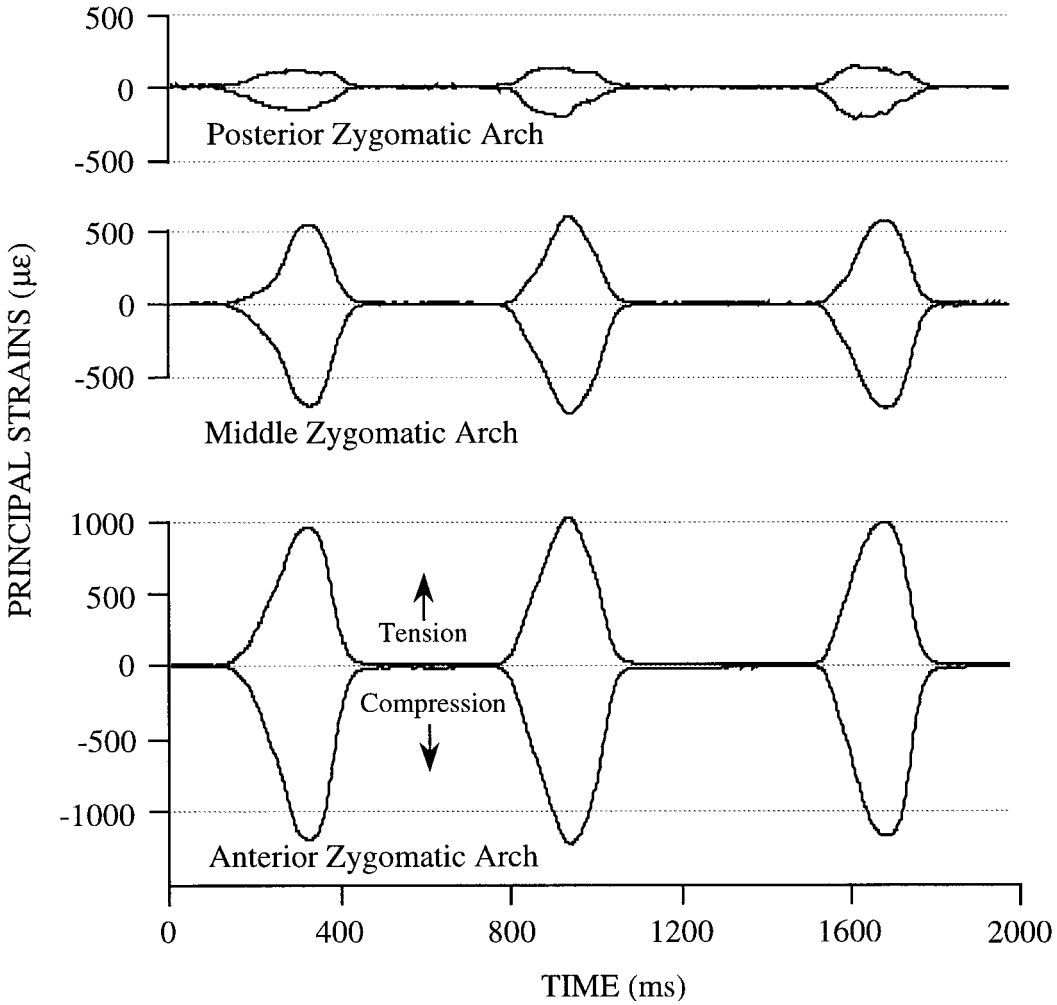

Fig. 4. Plot of the principal strains recorded simultaneously from the anterior, middle and posterior portions of the zygomatic arch of an adult female *Macaca fascicularis* during mastication. The zygomatic arch strains are from the right side and the subject is chewing a dried apricot on the same side. There are three power strokes in this figure. Note that the peak strains along the anterior portion of the zygomatic arch are much larger than those from the posterior portion. The strains from the middle portion tend to be more or less intermediate. See Figure 2 for location of the strain gages along the zygomatic arch.

the anterior, middle and posterior regions of the working-side zygomatic arch during mastication. As expected, peak strains occur during the power stroke. There are three power strokes in this figure and the subject is chewing a piece of dried apricot. Tables 1 and 2 indicate for both working and balancing sides the descriptive statistics for the peak principal strains and peak maximum shear strains (γmax) along these three regions of the zygomatic arch.

The data in Tables 1 and 2 indicate that strain magnitudes are ordinarily larger on the working side. In addition, strains recorded during the chewing of hard or tough objects are usually larger than those recorded during the chewing of apple skin. Finally, and most importantly, the anterior portion of the zygomatic arch experiences considerably more strain than does the posterior portion (Fig. 4). For example, Table 2 contains the values of γmax recorded from the anterior rosette divided by γmax values recorded from the posterior rosette. Based on the grand means of the four subjects for the chewing of hard or tough foods, there is

TABLE 1. Descriptive statistics for peak principal strains (ϵ_1 and ϵ_2) recorded from the zygomatic arch during the power stroke of mastication

Subject, food[1] and side	N	Anterior rosette						Middle rosette						Posterior rosette					
		ϵ_1			ϵ_2			ϵ_1			ϵ_2			ϵ_1			ϵ_2		
		Mean	(S.D.)	Largest	Mean	(S.D.)	Largest	Mean	(S.D.)	Largest	Mean	(S.D.)	Largest	Mean	(S.D.)	Largest	Mean	(S.D.)	Largest
Macaque 2																			
Monkey biscuit																			
working (l)	55	487	(54)	696	−464	(45)	−604	314	(46)	492	−507	(54)	−695	176	(33)	235	−151	(22)	−232
balancing (r)	62	320	(80)	522	−381	(103)	−645	197	(50)	342	−428	(84)	−648	183	(66)	354	−139	(44)	−258
Apple with skin																			
working (l)	36	510	(111)	726	−454	(89)	−623	337	(86)	510	−520	(95)	−700	143	(35)	218	−174	(37)	−249
balancing (r)	40	291	(49)	385	−365	(71)	−515	186	(36)	251	−393	(70)	−516	174	(46)	275	−123	(29)	−193
Macaque 5																			
Dried apricot																			
working (r)	41	623	(177)	1019	−731	(223)	−1236	293	(125)	603	−429	(140)	−760	127	(22)	176	−202	(35)	−276
balancing (l)	30	475	(119)	705	−769	(204)	−1194	261	(84)	417	−404	(108)	−629	198	(64)	358	−128	(45)	−239
Apple with skin																			
working (r)	32	524	(61)	631	−619	(71)	−753	240	(33)	308	−374	(46)	−470	129	(13)	144	−225	(16)	−241
balancing (l)	21	329	(95)	505	−512	(143)	−790	171	(55)	290	−270	(72)	−413	135	(38)	221	−83	(29)	−147
Macaque 7																			
Popcorn kernels																			
working (l)	41	431	(58)	628	−395	(59)	−591	264	(62)	447	−406	(75)	−654	222	(28)	319	−236	(29)	−337
balancing (r)	38	471	(110)	804	−454	(67)	−646	207	(51)	345	−401	(93)	−662	250	(46)	361	−273	(55)	−407
Apple with skin																			
working (l)	57	241	(66)	340	−198	(63)	−306	149	(39)	245	−249	(64)	−380	165	(42)	229	−192	(47)	−268
balancing (r)	39	269	(91)	457	−281	(92)	−458	127	(51)	235	−222	(82)	−391	126	(35)	211	−123	(44)	−219
Macaque 9																			
Monkey biscuit																			
working (r)	35	411	(59)	539	−396	(66)	−536	191	(26)	254	−273	(46)	−376	149	(11)	185	−152	(13)	−180
balancing (l)	46	356	(112)	586	−376	(117)	−628	129	(34)	205	−245	(69)	−389	88	(15)	120	−118	(29)	−184
Apple with skin																			
working (r)	22	323	(38)	388	−305	(40)	−388	169	(16)	194	−222	(23)	−266	131	(13)	154	−142	(11)	−161
balancing (l)	20	164	(75)	306	−180	(85)	−343	76	(27)	126	−126	(58)	−228	55	(13)	79	−62	(19)	−101
incision	7	428	(122)	586	−461	(128)	−616	158	(41)	205	−321	(84)	−424	153	(40)	205	−175	(50)	−242
Grand means																			
Hard/tough foods																			
Working		488	(87)		−497	(98)		266	(65)		−404	(79)		169	(24)		−185	(25)	
Balancing		406	(105)		−495	(123)		199	(55)		−370	(89)		180	(48)		−165	(43)	
Apple with skin																			
Working		400	(69)		−394	(66)		224	(44)		−341	(57)		142	(26)		−183	(28)	
Balancing		263	(78)		−335	(98)		140	(42)		−253	(71)		123	(33)		−98	(30)	

[1] Hard/tough foods includes monkey biscuit, dried apricot and popcorn kernels.
N is the number of chewing cycles; (l) or (r) indicates chewing on the left or right sides, respectively; (S.D.) is the standard deviation. Strain values are in microstrain units.

TABLE 2. Descriptive statistics for peak maximum shear strains (γmax) recorded from the zygomatic arch during the power stroke of mastication

Subject, food[1] and side	N	Anterior rosette γmax			Middle rosette γmax			Posterior rosette γmax			Ratio: Anterior γmax/ Posterior γmax	
		Mean	(S.D.)	Largest	Mean	(S.D.)	Largest	Mean	(S.D.)	Largest	Mean	(S.D.)
Macaque 2												
Monkey biscuit												
working (l)	55	951	(98)	1,300	821	(100)	1,187	328	(36)	413	2.9	(0.19)
balancing (r)	62	701	(183)	1,167	625	(134)	990	322	(109)	612	2.2	(0.20)
Apple with skin												
working (l)	36	964	(199)	1,328	857	(180)	1,202	316	(52)	416	3.1	(0.17)
balancing (r)	40	656	(119)	900	578	(106)	767	297	(74)	468	2.2	(0.21)
Macaque 5												
Dried apricot												
working (r)	41	1,354	(400)	2,256	721	(265)	1,363	329	(56)	448	4.1	(1.23)
balancing (l)	30	1,244	(322)	1,899	666	(190)	1,026	327	(109)	598	3.8	(0.43)
Apple with skin												
working (r)	32	1,143	(131)	1,385	614	(78)	778	354	(28)	382	3.2	(0.27)
balancing (l)	21	841	(237)	1,295	440	(127)	704	219	(67)	368	3.8	(0.35)
Macaque 7												
Popcorn kernels												
working (l)	41	826	(116)	1,218	670	(137)	1,101	458	(55)	656	1.8	(0.14)
balancing (r)	38	934	(214)	1,579	607	(144)	1,007	522	(101)	768	1.8	(0.14)
Apple with skin												
working (l)	57	439	(128)	632	398	(102)	625	357	(88)	496	1.2	(0.31)
balancing (r)	39	550	(183)	914	349	(132)	626	249	(87)	428	2.2	(0.28)
Macaque 9												
Monkey biscuit												
working (r)	35	807	(125)	1,075	464	(71)	630	301	(18)	344	2.7	(0.32)
balancing (l)	46	733	(229)	1,214	374	(103)	594	206	(44)	304	3.6	(0.44)
Apple with skin												
working (r)	22	628	(77)	776	391	(36)	460	273	(23)	316	2.3	(0.22)
balancing (l)	20	344	(160)	649	202	(84)	353	117	(32)	172	2.9	(0.61)
incision	7	889	(250)	1,202	480	(124)	629	328	(90)	442	2.7	(0.24)
Grand means												
Hard/tough foods												
Working		985	(185)		669	(143)		354	(41)		2.9	(0.47)
Balancing		903	(237)		568	(143)		344	(91)		2.9	(0.30)
Apple with skin												
Working		794	(134)		565	(99)		325	(48)		2.5	(0.24)
Balancing		598	(175)		392	(112)		221	(65)		2.8	(0.36)

[1] Hard/tough foods includes monkey biscuit, dried apricot and popcorn kernels.
N is the number of chewing cycles; (l) or (r) indicates chewing on the left or right sides, respectively; (S.D.) is the standard deviation. Strain values are in microstrain units.

about three times more strain anteriorly than posteriorly. Similarly, for chewing apple with skin, there is about two and a half times more strain anteriorly than posteriorly.

The data in Table 2 also demonstrate that the magnitude of γmax recorded from the middle rosette is intermediate to those values recorded from the anterior and posterior rosettes. Again, based on the grand means for the chewing of hard or tough food objects, there is nearly twice as much strain along the middle rosette than along the posterior rosette. Similarly, there is about 1.5 times more strain along the anterior rosette than along the middle rosette.

The data in Table 3 present the descriptive statistics for the subject (macaque 1) with only a single rosette positioned along the most anterior part of the arch. Similar to the other four subjects, during mastication the largest strains ordinarily occur along the working side. Most notable about this experiment, however, and in contrast to macaque 9, are the very large strains recorded during incision. For example, as much as $-2{,}113$ με in compression was recorded during incision of a whole unripe pear.

Strain direction

Table 4 presents the descriptive statistics for the angle ϕ during peak maximum shear strain (γmax). As noted earlier, this angle characterizes the direction of ϵ_1 (principal

TABLE 3. Descriptive statistics for peak strains (ϵ_1, ϵ_2 and γmax) and ϕ along the anterior portion of the zygomatic arch during the power stroke of mastication and incision

Subject, food and side	N	ϵ_1 Mean	ϵ_1 (S.D.)	ϵ_1 Largest	ϵ_2 Mean	ϵ_2 (S.D.)	ϵ_2 Largest	γmax Mean	γmax (S.D.)	γmax Largest	ϕ Mean	ϕ (S.D.)	ϕ Range
Macaque 1													
Hard unripe pear													
working (l)	26	518	(84)	763	−948	(136)	−1,321	1,466	(219)	2,083	48.1	(0.5)	47–49
incision	16	711	(314)	1,305	−1,207	(497)	−2,113	1,917	(810)	3,417	48.2	(1.0)	46–50
Apple with skin													
working (l)	29	618	(187)	841	−916	(279)	−1,201	1,534	(464)	2,042	46.5	(0.8)	45–49
balancing (r)	37	431	(113)	615	−760	(191)	−1,042	1,192	(304)	1,656	47.5	(0.6)	46–49
incision	8	709	(186)	1,015	−1,262	(313)	−1,773	1,970	(498)	2,789	48.9	(0.5)	48–50

Strain values are in microstrain units; ϕ is in degrees relative to the long axis of the zygomatic arch (see Fig. 3).
N is the number of chewing cycles; (l) or (r) indicates chewing on the left or right sides, respectively; (S.D.) is the standard deviation.
This subject did not chew pear on the right side.

tension) relative to the long axis of the zygomatic arch (Fig. 3). Figure 5 indicates the mean direction of ϵ_1 for each individual subject, whereas Figure 6 indicates the overall mean direction of ϵ_1 for all subjects combined. These data indicate that along the anterior and middle rosettes, the direction of ϵ_1 during peak strain is upwards and anterior (or downwards and posterior), and along the posterior rosette it is upwards and posterior (or downwards and anterior). The lone exception to this pattern is for working-side strain along the posterior rosette in macaque 5, where ϵ_1 is directed primarily upwards and slightly rostral, rather than upwards and caudal. The data in Table 4 and Figures 5 and 6 also indicate that within each subject and for any given rosette position, at peak shear strain ϕ is almost always larger along the balancing side.

There were also certain alternating patterns in values of ϕ during loading and unloading along both working and balancing sides. Throughout the power stroke, values of ϕ generally increase along the working side and decrease along the balancing side. Although the data in Table 4 and Figure 7 demonstrate this trend only for peak strain and for 25% of peak strain during loading and unloading, the values of ϕ for the 50% and 75% levels of peak strain also fit this pattern.

As seen in Figure 7, compared to the anterior rosette, for the middle and posterior rosettes there tends to be a larger difference in average values of ϕ between 25% of peak strain during loading and during unloading. For the anterior rosette there is, on average, about a 9-degree difference in these values, whereas for the middle and posterior rosettes there is, on average, about a 25- to 30-degree difference (Table 4).

Finally, for the subject with a single rosette along its arch, Table 3 presents the descriptive statistics for the angle ϕ during peak γmax. Overall, these angles are very similar to the data presented in Table 4 and Figures 5 and 6. Furthermore, there was very little difference between incision, working- and balancing-side values.

Values of ϵ_1/ϵ_2

Table 5 indicates the descriptive statistics for the values ϵ_1/ϵ_2 during the power stroke of mastication. Similar to the values of ϕ, there are certain differences associated with the three rosette positions. For example, the smallest ratio values during peak strain are consistently found along the middle rosette. Whereas the values along the middle rosette are usually well below 1.0, the values along the anterior and posterior rosettes are often closer to or even larger than 1.0. Thus, whereas compressive strain (ϵ_2) is often much larger than tensile strain (ϵ_1) along the middle rosette, tensile strain is often only slightly smaller, near equal, or even somewhat larger than compressive strain along the anterior and posterior rosettes.

There are also consistent differences between the working- and balancing-side ϵ_1/ϵ_2 values during peak strain. For the anterior and middle rosettes, the largest average values are along the working side, whereas for the posterior rosette the largest values are most often along the balancing side.

Again, similar to values of ϕ, there were certain alternating patterns in values of ϵ_1/ϵ_2 during loading and unloading (Table 5).

TABLE 4. Descriptive statistics for the angle ϕ along the zygomatic arch during peak shear strain (γmax) and during 25% of peak γmax for loading and unloading

Subject, food and side	N	Anterior rosette						Middle rosette						Posterior rosette					
		Load (25%)		Peak (100%)		Unload (25%)		Load (25%)		Peak (100%)		Unload (25%)		Load (25%)		Peak (100%)		Unload (25%)	
		Mean	(S.D.)	Mean	(S.D.)	Mean	(S.D.)	Mean	(S.D.)	Mean	(S.D.)	Mean	(S.D.)	Mean	(S.D.)	Mean	(S.D.)	Mean	(S.D.)
Macaque 2																			
Monkey biscuit																			
working (l)	55	41.5	(2.6)	53.2	(1.2)	58.4	(5.1)	58.4	(1.9)	75.1	(1.2)	78.5	(5.5)	118.1	(3.9)	153.8	(11.4)	162.8	(14.6)
balancing (r)	62	64.5	(2.2)	58.9	(1.2)	49.5	(7.8)	90.2	(2.0)	84.2	(1.9)	71.7	(9.8)	173.6	(1.0)	163.8	(4.7)	127.5	(19.3)
Apple with skin																			
working (l)	36	42.3	(1.8)	50.9	(1.5)	56.7	(6.0)	59.7	(1.9)	73.3	(2.0)	79.2	(5.7)	118.5	(2.3)	140.2	(13.9)	159.4	(16.5)
balancing (r)	40	64.4	(1.8)	60.2	(1.3)	51.3	(7.0)	87.6	(1.7)	83.8	(2.2)	73.2	(8.9)	172.7	(1.4)	166.6	(3.4)	129.8	(15.8)
Macaque 5																			
Dried apricot																			
working (r)	41	49.6	(3.8)	52.8	(1.2)	58.7	(5.3)	44.1	(6.3)	55.8	(2.9)	68.0	(11.4)	61.0	(7.1)	66.0	(4.3)	118.6	(22.1)
balancing (l)	30	66.0	(1.9)	60.5	(1.0)	53.7	(5.8)	90.2	(4.3)	72.8	(3.4)	59.2	(11.0)	133.1	(5.2)	136.8	(1.2)	105.4	(27.2)
Apple with skin																			
working (r)	32	46.3	(1.0)	53.0	(0.8)	58.9	(1.8)	43.0	(1.4)	56.1	(2.7)	70.2	(3.0)	68.4	(3.2)	74.6	(1.6)	112.5	(17.5)
balancing (l)	21	66.4	(2.4)	61.1	(1.8)	54.0	(9.3)	87.5	(4.7)	74.5	(3.6)	61.1	(16.1)	143.0	(4.7)	150.2	(2.0)	108.3	(35.2)
Macaque 7																			
Popcorn kernels																			
working (l)	41	49.3	(2.2)	54.0	(0.9)	54.0	(3.0)	46.5	(5.4)	73.7	(4.5)	74.2	(11.7)	136.8	(2.7)	139.6	(1.2)	148.4	(4.3)
balancing (r)	38	58.6	(0.8)	55.0	(1.0)	54.3	(4.3)	86.2	(3.5)	68.4	(3.3)	60.7	(10.7)	141.4	(2.7)	138.2	(1.0)	145.3	(3.7)
Apple with skin																			
working (l)	57	41.5	(6.4)	49.7	(4.3)	37.8	(17.1)	45.7	(9.4)	57.8	(8.1)	54.2	(17.1)	140.4	(3.4)	137.8	(1.2)	148.7	(4.3)
balancing (r)	39	58.5	(2.0)	57.8	(0.9)	54.1	(4.2)	85.3	(9.5)	78.3	(4.3)	65.1	(19.1)	150.3	(4.6)	142.0	(1.9)	152.7	(7.0)
Macaque 9																			
Monkey biscuit																			
working (r)	35	51.4	(3.1)	59.6	(1.0)	63.8	(1.9)	46.1	(5.4)	66.4	(5.7)	86.1	(3.9)	128.9	(5.2)	136.5	(3.7)	164.2	(3.3)
balancing (l)	46	65.5	(1.2)	61.9	(0.4)	59.6	(5.0)	93.8	(4.1)	85.1	(4.2)	66.9	(5.0)	166.7	(5.4)	149.4	(2.2)	146.9	(9.2)
Apple with skin																			
working (r)	22	48.1	(2.5)	58.9	(1.0)	62.0	(1.3)	45.4	(4.1)	56.9	(3.3)	87.2	(4.2)	126.4	(4.3)	133.0	(1.6)	168.0	(5.0)
balancing (l)	20	70.0	(2.5)	65.7	(1.5)	53.2	(15.8)	93.0	(6.7)	83.1	(17.4)	58.9	(16.4)	175.6	(6.1)	157.6	(10.5)	140.5	(13.2)
incision	7	66.0	(1.1)	63.0	(1.1)	64.9	(1.5)	93.7	(6.0)	86.0	(4.2)	74.7	(7.5)	158.7	(2.9)	150.4	(2.3)	162.7	(2.9)
Grand means																			
Hard/tough foods																			
working		48.0	(2.9)	54.9	(1.1)	58.7	(3.8)	48.8	(4.8)	67.8	(3.6)	76.7	(8.1)	111.2	(4.7)	124.0	(5.2)	148.5	(11.1)
balancing		63.7	(1.5)	59.1	(0.9)	54.3	(5.7)	90.1	(3.5)	77.6	(3.2)	64.6	(9.1)	153.7	(3.6)	147.1	(2.3)	131.3	(14.9)
Apple with skin																			
working		44.6	(2.9)	53.1	(1.9)	53.9	(6.6)	48.5	(4.2)	61.0	(4.0)	72.7	(7.5)	113.4	(3.3)	121.4	(4.6)	147.2	(10.8)
balancing		64.8	(2.2)	61.2	(1.4)	53.2	(9.1)	88.4	(5.7)	79.9	(6.9)	64.6	(15.1)	160.4	(4.2)	154.1	(4.5)	132.8	(17.8)

ϕ is in degrees relative to the long axis of the zygomatic arch (see Figs. 3, 5, and 6).
Hard/tough foods includes monkey biscuit, dried apricot and popcorn kernels.
N is the number of chewing cycles; (l) or (r) indicates chewing on the left or right sides, respectively; (S.D.) is the standard deviation.

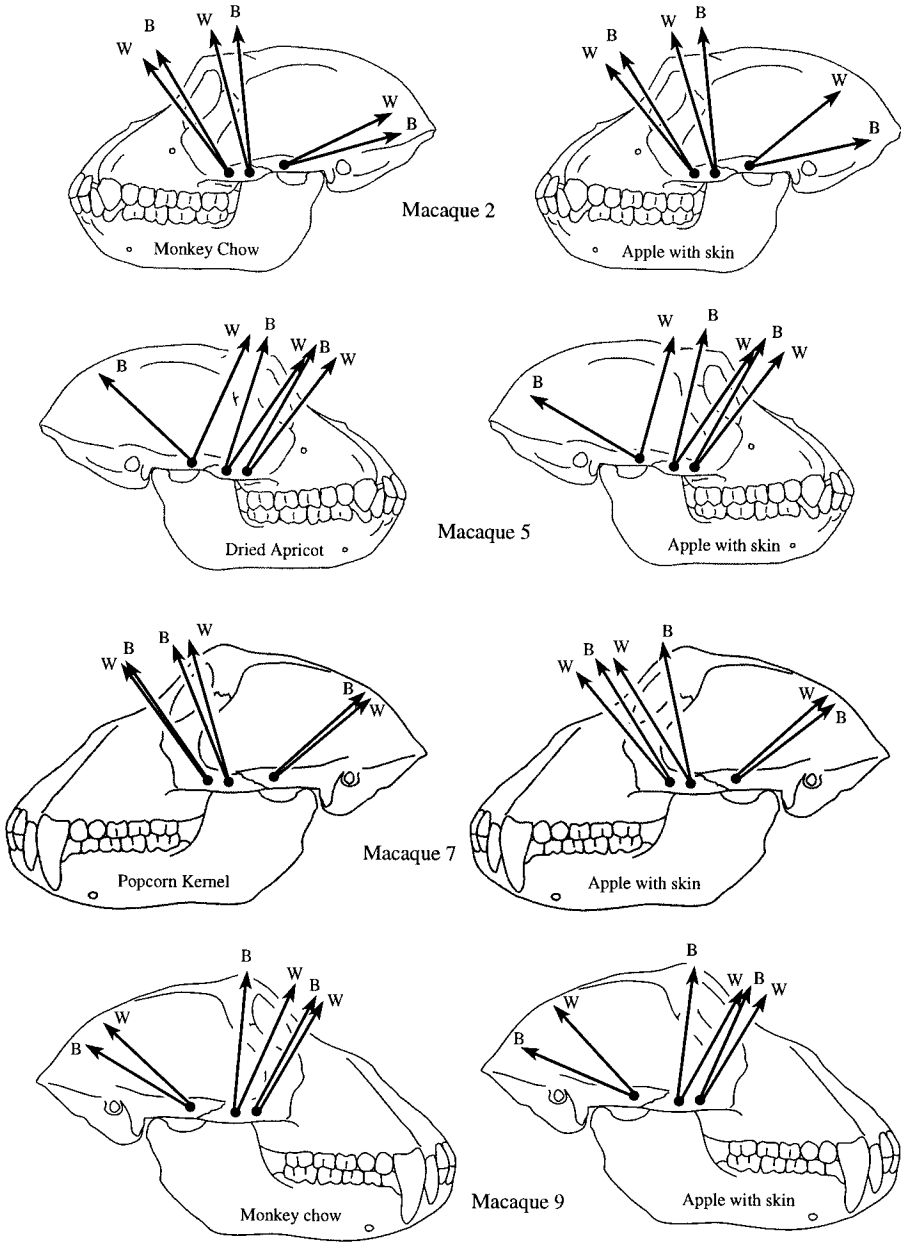

Fig. 5. The arrows indicate the average direction of ϵ_1 at peak zygomatic arch strain for each of the four subjects when chewing hard/tough food objects and apple with skin. For each rosette, W indicates working-side strains and B indicates balancing-side strains.

For the working-side rosettes, these values during the power stroke tend to decrease along the anterior and middle rosettes and increase along the posterior rosette. For the balancing-side rosettes, the reverse situation prevails. Furthermore, for both working and balancing sides, the largest ratio changes throughout the power stroke occur along the posterior rosette, while the smallest changes occur along the middle rosette.

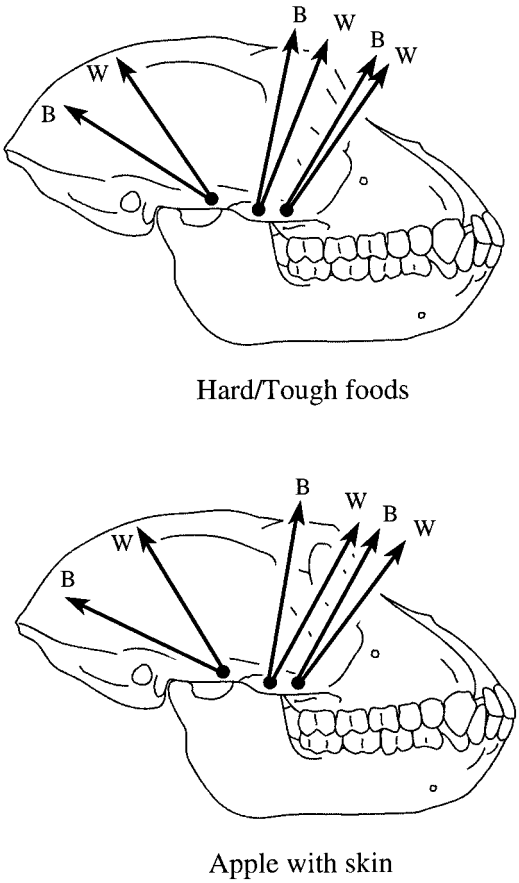

Fig. 6. The arrows indicate the average direction of ϵ_1 at peak zygomatic arch strain for all subjects combined when chewing hard/tough food objects and apple with skin. For each rosette, W indicates working-side strains and B indicates balancing-side strains.

DISCUSSION

Strain gradients in the zygomatic arch andthe optimal design of facial bones

It was originally expected that in vivo bone strain magnitudes during mastication and biting would be more or less similar throughout different regions of the facial skeleton (Hylander et al., 1987, 1991). This expectation was based largely on the well-known fact that loading conditions play an important role in the maintenance of bone mass (Liskova and Hert, 1971; Morey and Baylink, 1978; Bouvier and Hylander, 1981; Lanyon and Rubin, 1985; Kimmel, 1993). This ability of bone to respond to cyclical mechanical loading, which is often called "functional adaptation" (e.g., Roux, 1881; Murray, 1936; Kummer, 1972; Goodship et al., 1979; Lanyon and Rubin, 1985; Martin and Burr, 1989), is thought to have the effect of maintaining bone strain magnitudes within a particular range of values, e.g., the "optimal strain environment" of Rubin (1984) and Lanyon and Rubin (1985; also cf. Bassett, 1968; Kummer, 1972; Pauwels, 1980; Lanyon et al., 1982; Lanyon, 1991). Thus, this concept of how bone responds to routine cyclical loads leads to the belief that there must be a more or less uniform distribution of functional strain throughout the bony face (Fig. 1), and moreover, that facial bones are optimized for countering masticatory loads, i.e., that they exhibit minimum material and maximum strength for countering routine cyclical loading regimes (cf. Roberts et al., 1992).

At this point, it may be useful to consider the definition of the "optimal strain environment." Although the optimal strain environment was not precisely defined by Rubin and Lanyon, it is clear that these authors consider peak functional principal strains to be an important component of this environment (Rubin, 1984; Rubin and Lanyon, 1984; Lanyon and Rubin, 1985). For example, while discussing their "dynamic strain similarity model," Lanyon and Rubin have repeatedly pointed out that peak functional strains within vertebrates tend to lie within the 2,000 to 3,000 με level. This means that for load-bearing bones, natural selection "has produced a margin of safety between functional and yield strains of between two and three times" (Rubin and Lanyon, 1984:323). On the other hand, it is also clear that these authors (and many others as well) do not believe that peak functional strains are necessarily the only or even the most important of the various physical stimuli that have osteoregulatory capabilities (cf. Lanyon and Rubin, 1985; Martin and Burr, 1989; Rubin et al., 1994). As recently pointed out by Rubin et al. (1994), strain magnitude, the fabric tensor, strain frequency, strain rate, strain gradients, electrokinetics, piezoelectricity, strain history, strain energy density, etc. have all been thought to be important osteoregulatory stimuli. Thus, we interpret

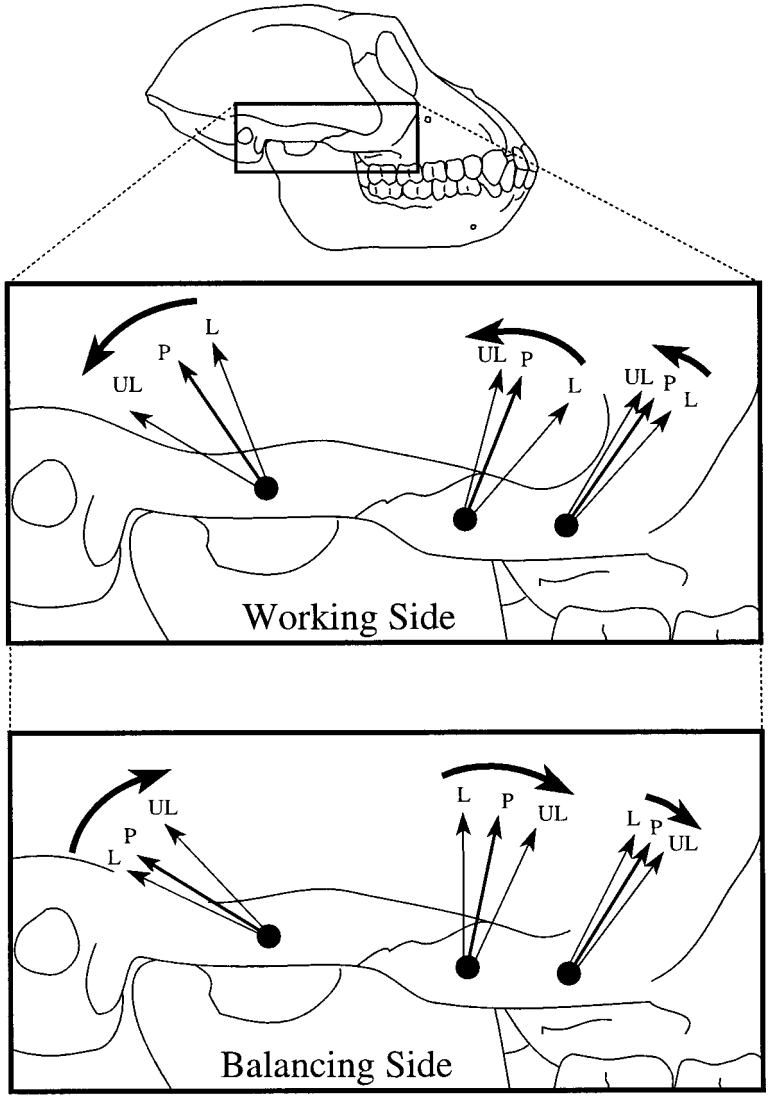

Fig. 7. The straight arrows indicate the average direction of ϵ_1 at peak zygomatic arch strain (P) and 25% of peak strain during loading (L) and unloading (UL) for all subjects combined when chewing hard/tough food objects. The large curved arrows indicate the progressive changes in the direction of ϵ_1 during loading and unloading throughout the power stroke. Note that on the working side the average direction of ϵ_1 changes in a counterclockwise direction, whereas on the balancing side the reverse condition prevails. The clockwise and counterclockwise patterns are reversed for the left zygomatic arch.

the concept of the optimal strain environment as simply meaning that peak principal strains for load-bearing bones will be about 2,000–3,000 με during strenuous but routine behaviors, and certainly will not regularly exceed these limits. If they did exceed these limits, there would be a greatly increased risk of bone failure during routine functional behaviors. It is for this reason that our study focuses on peak strain magnitudes, and not because we believe that they are necessarily an osteoregulatory stimulus of overriding importance. On the other hand, peak strain magnitudes presumably are

TABLE 5. Descriptive statistics for the ratio ϵ_1/ϵ_2 along the zygomatic arch during peak shear strain (γmax) and during 25% of peak γmax for loading and unloading

Subject, food and side	N	Anterior rosette						Middle rosette						Posterior rosette					
		Load (25%)		Peak (100%)		Unload (25%)		Load (25%)		Peak (100%)		Unload (25%)		Load (25%)		Peak (100%)		Unload (25%)	
		Mean	(S.D.)	Mean	(S.D.)	Mean	(S.D.)	Mean	(S.D.)	Mean	(S.D.)	Mean	(S.D.)	Mean	(S.D.)	Mean	(S.D.)	Mean	(S.D.)
Macaque 2																			
Monkey biscuit																			
working (l)	55	1.41	(0.13)	1.05	(0.04)	0.91	(0.20)	0.82	(0.03)	0.62	(0.02)	0.57	(0.06)	0.56	(0.04)	1.19	(0.26)	1.46	(0.36)
balancing (r)	62	0.73	(0.03)	0.84	(0.03)	1.18	(0.22)	0.45	(0.03)	0.46	(0.03)	0.56	(0.11)	1.67	(0.08)	1.30	(0.12)	0.62	(0.30)
Apple with skin																			
working (l)	36	1.40	(0.09)	1.12	(0.06)	0.94	(0.22)	0.78	(0.03)	0.64	(0.05)	0.57	(0.06)	0.54	(0.04)	0.86	(0.28)	1.35	(0.37)
balancing (r)	40	0.68	(0.05)	0.80	(0.04)	1.04	(0.22)	0.47	(0.03)	0.47	(0.01)	0.54	(0.07)	1.77	(0.17)	1.40	(0.10)	0.66	(0.18)
Macaque 5																			
Dried apricot																			
working (r)	41	1.03	(0.13)	0.86	(0.04)	0.73	(0.17)	0.65	(0.13)	0.67	(0.06)	0.62	(0.15)	0.66	(0.12)	0.63	(0.04)	1.20	(0.44)
balancing (l)	30	0.57	(0.02)	0.62	(0.01)	0.77	(0.15)	0.54	(0.03)	0.64	(0.06)	0.63	(0.12)	1.68	(0.30)	1.56	(0.06)	1.17	(0.55)
Apple with skin																			
working (r)	32	1.04	(0.06)	0.85	(0.03)	0.67	(0.05)	0.74	(0.04)	0.64	(0.02)	0.60	(0.05)	0.50	(0.10)	0.57	(0.04)	0.64	(0.28)
balancing (l)	21	0.61	(0.03)	0.64	(0.03)	0.86	(0.22)	0.69	(0.07)	0.63	(0.04)	0.79	(0.17)	2.49	(1.28)	1.67	(0.21)	1.52	(1.69)
Macaque 7																			
Popcorn kernels																			
working (l)	41	1.28	(0.13)	1.10	(0.04)	1.27	(0.15)	0.61	(0.06)	0.64	(0.04)	0.72	(0.12)	0.93	(0.11)	0.94	(0.03)	1.28	(0.24)
balancing (r)	38	0.91	(0.04)	1.02	(0.03)	1.13	(0.16)	0.55	(0.06)	0.51	(0.02)	0.55	(0.06)	1.16	(0.15)	0.92	(0.03)	1.05	(0.20)
Apple with skin																			
working (l)	57	1.42	(0.21)	1.25	(0.16)	1.83	(0.78)	0.70	(0.09)	0.60	(0.03)	0.76	(0.23)	0.94	(0.26)	0.86	(0.06)	0.98	(0.23)
balancing (r)	39	0.94	(0.09)	0.95	(0.03)	1.15	(0.17)	0.73	(0.31)	0.57	(0.06)	0.78	(0.31)	2.07	(3.67)	1.03	(0.12)	1.36	(0.90)
Macaque 9																			
Monkey biscuit																			
working (r)	35	1.38	(0.16)	1.04	(0.03)	0.92	(0.08)	0.95	(0.12)	0.70	(0.04)	0.72	(0.07)	1.39	(0.88)	0.98	(0.11)	1.47	(0.82)
balancing (l)	46	0.87	(0.04)	0.95	(0.01)	0.92	(0.09)	0.52	(0.04)	0.53	(0.02)	0.75	(0.14)	1.25	(0.41)	0.76	(0.10)	1.48	(0.79)
Apple with skin																			
working (r)	22	1.39	(0.12)	1.06	(0.03)	0.92	(0.05)	1.00	(0.11)	0.77	(0.06)	0.71	(0.08)	1.13	(0.28)	0.92	(0.05)	1.02	(0.25)
balancing (l)	20	0.96	(0.15)	0.91	(0.04)	1.51	(0.95)	0.65	(0.16)	0.64	(0.16)	1.41	(1.32)	1.76	(0.86)	0.92	(0.17)	1.68	(0.90)
incision	7	0.90	(0.02)	0.93	(0.02)	0.88	(0.04)	0.55	(0.13)	0.49	(0.03)	0.56	(0.11)	1.35	(0.47)	0.88	(0.08)	1.42	(0.15)
Grand means																			
Hard/tough foods																			
working		1.28	(0.14)	1.01	(0.04)	0.96	(0.15)	0.76	(0.09)	0.66	(0.04)	0.66	(0.10)	0.89	(0.29)	0.94	(0.11)	1.35	(0.47)
balancing		0.77	(0.03)	0.86	(0.02)	1.00	(0.16)	0.52	(0.04)	0.54	(0.03)	0.62	(0.11)	1.44	(0.24)	1.14	(0.08)	1.08	(0.46)
Apple with skin																			
working		1.31	(0.12)	1.07	(0.07)	1.09	(0.28)	0.81	(0.07)	0.66	(0.04)	0.66	(0.11)	0.78	(0.17)	0.80	(0.11)	1.00	(0.28)
balancing		0.80	(0.08)	0.83	(0.04)	1.14	(0.39)	0.64	(0.14)	0.58	(0.07)	0.88	(0.47)	2.02	(1.50)	1.26	(0.15)	1.31	(0.92)

Hard/tough foods includes monkey biscuit, dried apricot and popcorn kernels.
N is the number of chewing cycles; (l) or (r) indicates chewing on the left or right sides, respectively; (S.D.) is the standard deviation.

linked or correlated with many of the above mentioned stimuli.

The in vivo bone strain data recorded in both this study on the zygomatic arch and in our earlier work on mandible and browridges demonstrate that peak functional strains differ greatly from one region of the bony face to the next (cf. Hylander et al., 1991). The zygomatic arch data indicate that the anterior portion of the arch experiences on average almost three times more strain than does the posterior portion, although as noted in the introduction, even greater differences in strain magnitudes exist throughout other areas of the face. For example, during chewing and biting, both the macaque mandibular corpus and anterior portion of the zygomatic arch experience about 20 times more strain than does the rostral interorbital region. Finally, relative to the optimal strain environment of Rubin and Lanyon (1994), peak principal strains in the high-strain areas of the face occasionally are indeed in the neighborhood of 2,000 με. On the other hand, peak strains in other areas are always well below these values.

In summary, the fact that the overall magnitude of peak functional strains is highly variable from one region of the skull to the next indicates that it is unlikely that all facial bones are especially designed to minimize bone tissue and maximize strength for countering masticatory loads. As we have argued elsewhere (Hylander et al., 1991; Hylander and Johnson, 1992), the apparent concentration of bone mass within certain regions of the face need not necessarily bear any relationship to the presence of large routine masticatory loads.

Finally, it is of interest to note that as early as 1984 it was hypothesized that the cranium may not be influenced by "functional adaptation," and instead its morphological state is perhaps entirely genetically determined, i.e., it lies along the genetic baseline of Figure 1 (Rubin, 1984). Implicit in this hypothesis is that functional strains must be very low in the cranium during chewing and biting. Although an in vivo bone strain analysis of macaque and baboon browridges tends to support this hypothesis (Hylander et al., 1991), an analysis of strain in the zygomatic arch and anterior root of the zygoma does not. Similarly, it has been asserted by Carter (1987:1095) that . . . "Bones which form by intramembranous ossification, such as the skull bones, tend to maintain their form and mass throughout adult life, even though they experience negligible mechanical loading during daily activities." Our analyses of the mandible and zygoma clearly refute Carter's assertion that all skull bones experience negligible mechanical loading (Hylander, 1979c, 1984), and also demonstrate that mode of bone formation (intramembranous vs. endochondral) tells us little about "mechanical loading during daily activities." Furthermore, Bouvier and Hylander's work (1981) on the macaque mandible, a bone formed largely by "intramembranous ossification," demonstrate the importance of mechanical loading for bone growth and maintenance.

Bone strain levels and morphology

Based on known levels of functional strains, what sorts of predictions, if any, can be made regarding the distribution of bone mass within the craniofacial region of macaques? As already noted, the posterior portion of the zygomatic arch experiences much less strain than does the anterior portion. Although the external dimensions of the macaque zygomatic arch do differ somewhat between anterior and posterior portions, what about the distribution of cortical and trabecular bone within these areas? If forces and moments associated with the masseter muscle were evenly distributed along the entire zygomatic arch, one would predict that the low strains from the posterior portion of the arch are due to its being much stiffer than the anterior portion, and if so, this must be because of much larger external dimensions and/or a much denser concentration of bone mass posteriorly. However, most of the masseter muscle is concentrated along the anterior part of the arch, and as to be discussed in a later section, because the zygomatic arch has fixed ends, shearing forces and bending and twisting moments along the arch are not evenly distributed, and instead are larger anteriorly. Therefore, *perhaps there is no difference in the overall internal architecture of the anterior and*

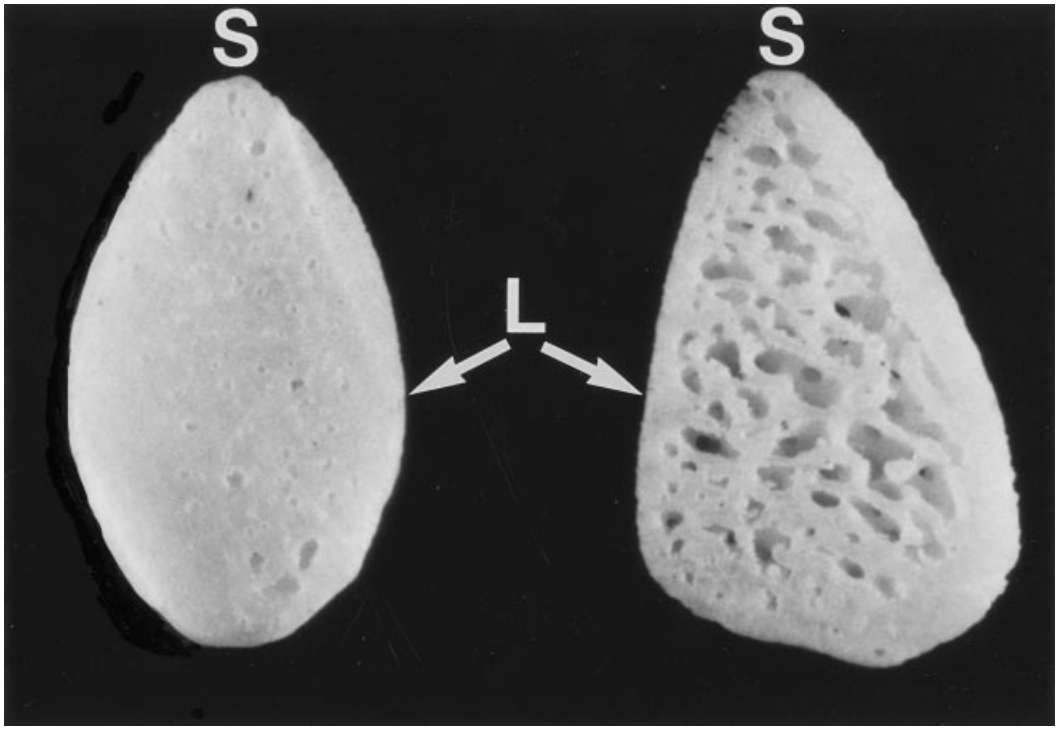

Fig. 8. Photographs of cross-sections of the left zygomatic arch of a large adult male *Macaca fascicularis* (WLH private collection). L and S indicate the lateral and superior surfaces of the arch, respectively. The section on the left is from the anterior portion of the zygomatic arch and the section on the right is from the posterior portion. The anterior section is almost all compact bone, whereas the posterior section has a considerable amount of trabecular bone.

posterior portions of the arch, and the differences in functional strains are due simply to the more anteriorly positioned muscle force and larger moments along the anterior part of the arch.

Cross-sections of the macaque zygomatic arch do not support either of these expectations, i.e., either a stiffer posterior portion or no difference in stiffness between anterior and posterior portions. As demonstrated in Figure 8, whereas the oval anterior portion of the arch is near solid cortical bone, the more triangular posterior portion is made up of trabecular bone surrounded by a relatively thin layer of cortical bone. Furthermore, the cortical bone is particularly thin along the lateral aspect of the zygomatic arch, which is the location from where the strains were recorded. Thus, although functional strains are much smaller along the posterior portion of the arch, there is also much less bone mass in this area. If the density of bone mass was comparable to what is found anteriorly, there would be even less strain posteriorly.

Do these results indicate that low-strain areas in the face will always be characterized by trabecular bone surrounded by a thin layer of cortical bone? A consideration of strain along and morphology of the rostral interorbital region indicates that this is not the case. Although functional strain levels along the rostral interorbital region are lower than in any other area yet examined by us (Hylander et al., 1991), this area is made up of a very thick dense layer of cortical bone (Fig. 9). Furthermore, and contrary to Lanyon (1991), these observations make it quite unlikely that bone mass is strictly determined by peak functional strains. Instead, as noted by many workers, the heritability of bone mass appears to be near 70 to 80% (e.g., Slemenda et al., 1991; Morrison et al., 1994).

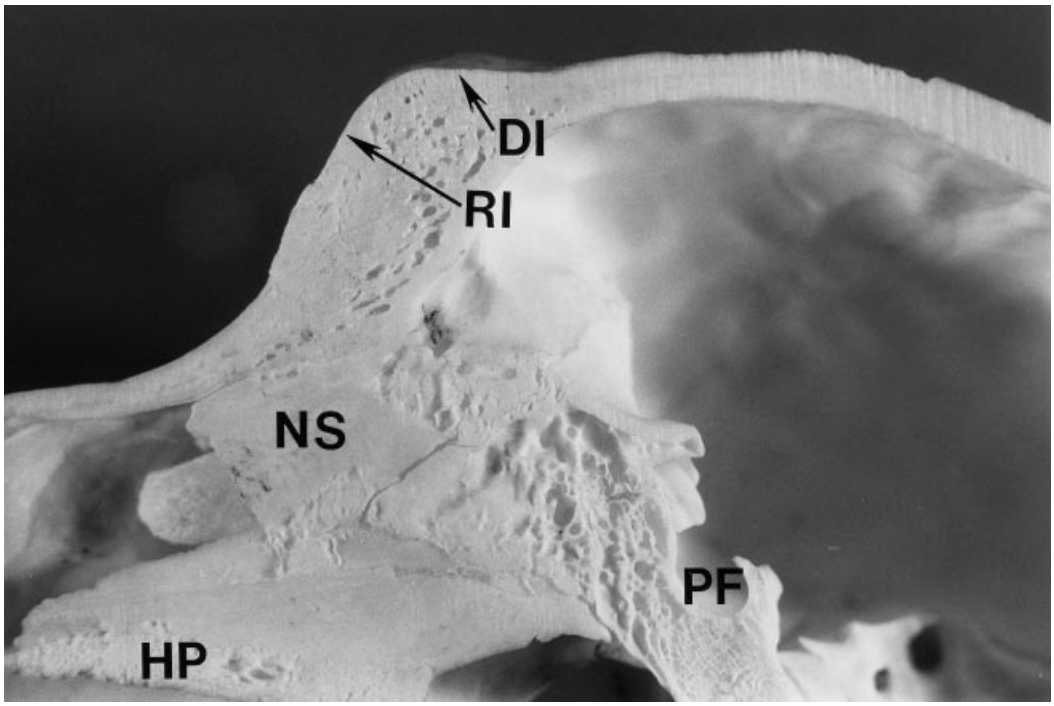

Fig. 9. Photograph of a midsagittal section of the skull of a large adult male *Macaca fascicularis* (WLH private collection). Abbreviations: rostral interorbital region (RI); dorsal interorbital region (DI); pituitary fossa (PF); nasal septum (NS), and hard palate (HP). Note that although the RI experiences relatively small functional strains during chewing and biting, this region has a large amount of solid cortical bone. Also note that the cranial base immediately rostral to the PF has a very sparse distribution of trabecular bone.

What about the architectural correlates of high-strain areas? Levels of functional strains are relatively high in the mandibular corpus and symphysis, anterior root of the zygoma, and anterior portion of the zygomatic arch, and these areas also exhibit relatively thick areas of densely compacted cortical bone (e.g., Fig. 2 in Hylander, 1979a; and Fig. 8). As certain areas of the face may not conform to this pattern (cf. Ward, 1991), and until functional strains have been recorded in the upper jaw, it is premature to conclude that high-strain areas in the craniofacial region are always associated with a thick layer of dense cortical bone. Thus, although high levels of strain may or may not always be associated with densely compacted cortical bone, the presence of low levels of strain clearly does not allow one to predict anything about the internal architecture of the underlying bone. Why is this so?

As previously noted, during chewing and biting, certain areas of the face experience relatively high functional strains. Moreover, these same areas are made up primarily of dense cortical bone. If bone mass in these areas was to be uniformly reduced by about 30–40% (as in the reduction in bone mass from the anterior to posterior portion of the zygomatic arch), functional strain levels during powerful chewing and biting would increase and perhaps reach dangerously high levels. Thus, it can be argued that the geometry and density of bone mass in the relatively high-strain areas are importantly related to countering masticatory loads (Hylander et al., 1991), and if an allowance is made for an appropriate safety factor (cf., Alexander, 1981; Rubin, 1984; Currey, 1984; Lanyon and Rubin, 1984; Biewener, 1993), then these areas may function in part as near optimized structures for countering masticatory forces. This of course does not mean that the entire bone is optimized for load-bearing, e.g., significant portions of the macaque mandibular corpus are not ex-

posed to relatively large bending and twisting moments during chewing and biting (Daegling, 1993).

But what about the low-strain areas such as the posterior portion of the zygomatic arch, browridge, and the rostral interorbital region? Why has there not been selection to *reduce* the bone mass in these regions? Although functional strains during chewing and biting might double or triple in magnitude following such a reduction, these regions would still be strong enough to counter masticatory loads, and they would more closely approximate the optimal and presumably desirable condition of maximum strength with minimum material for countering chewing and biting.

Perhaps one reason why bone mass has not been further reduced is simply because facial bones must *also* be structurally adapted to counter infrequent nonmasticatory traumatic loads. For example, although a significant reduction in bone mass of the posterior portion of the zygomatic arch would have little bearing on its continued structural competence for countering routine masticatory loads, this reduction would surely weaken this region to blows delivered to the orbit and zygomatic arch, and of course for most mammals a broken zygomaxillary complex would seriously diminish an individual's overall reproductive fitness because of its decreased ability to nourish itself due to a painful and malfunctioning masticatory apparatus. A similar argument can be made for the browridge and interorbital region, although structural failure in these instances does not result in a malfunctioning masticatory apparatus, but instead may result in damage to the contents of the orbit or neurocranium (cf. Hylander et al., 1991).

Safety factors and structural failure of the facial skeleton

An interesting finding in our work relates to the peak levels of recorded strain. As indicated in Table 3, compressive strain magnitudes as high as $-2{,}113$ με have been recorded from the zygomatic arch during powerful biting. Furthermore, as much as 2,155 με in tension was recorded from the anterior root of the zygoma of a macaque that engaged in powerful biting (Hylander and Johnson, in prep.). Comparable levels of compressive strain during biting have been recorded in the mandibular corpus of galagos and macaques (i.e., -2164 με and -1537 με, respectively; Hylander, 1979c). These data are interesting, as bone strain magnitudes in the range of -2000 to -3000 με appear to be near the upper limit of functional strains that occur in vertebrates during normal routine behaviors (Rubin, 1984; Lanyon and Rubin, 1985). This strain limit is thought to be importantly related to factors of safety in the design of skeletal tissues.

If safety factors to minimize traumatic injuries are built into craniofacial structures, what is the nature of these factors? Unlike various postcranial bones that occasionally fail due to fatigue fractures during vigorous or increased levels of locomotor activity (cf. Nunamaker et al., 1990), with the possible exception of pathological fractures associated with tumors or cysts, we are unaware of any instances where facial bones have experienced structural failure during chewing and biting. This suggests that not all bones have the same safety factor for countering routine cyclical loads (cf. Alexander, 1981; Rubin, 1984; Lanyon and Rubin, 1985; Biewener, 1993). This is hardly surprising, as the consequences of fractured bones must vary considerably. For example, for highly active mammals a fractured rib is ordinarily less of a problem than is a broken femur or mandible. In fact, healed rib fractures are a common occurrence among wild-shot great apes, whereas healed femoral fractures are less commonly found and healed mandibular fractures are absent or extremely rare (Lovell, 1990).

An important reason for this distribution of healed fractures, of course, is that apes with mandibular and femoral fractures are less apt to survive long enough for the fracture to heal, and therefore are less apt to be included in these wild-shot study samples. If they are less apt to survive, then it is also likely that natural selection has resulted in the safety factors for the femur and mandible to be significantly larger than those for ribs, and therefore a fractured mandible or femur is also less apt to occur. Furthermore, if safety factors do differ from one bone to the next and if the development of safety factors

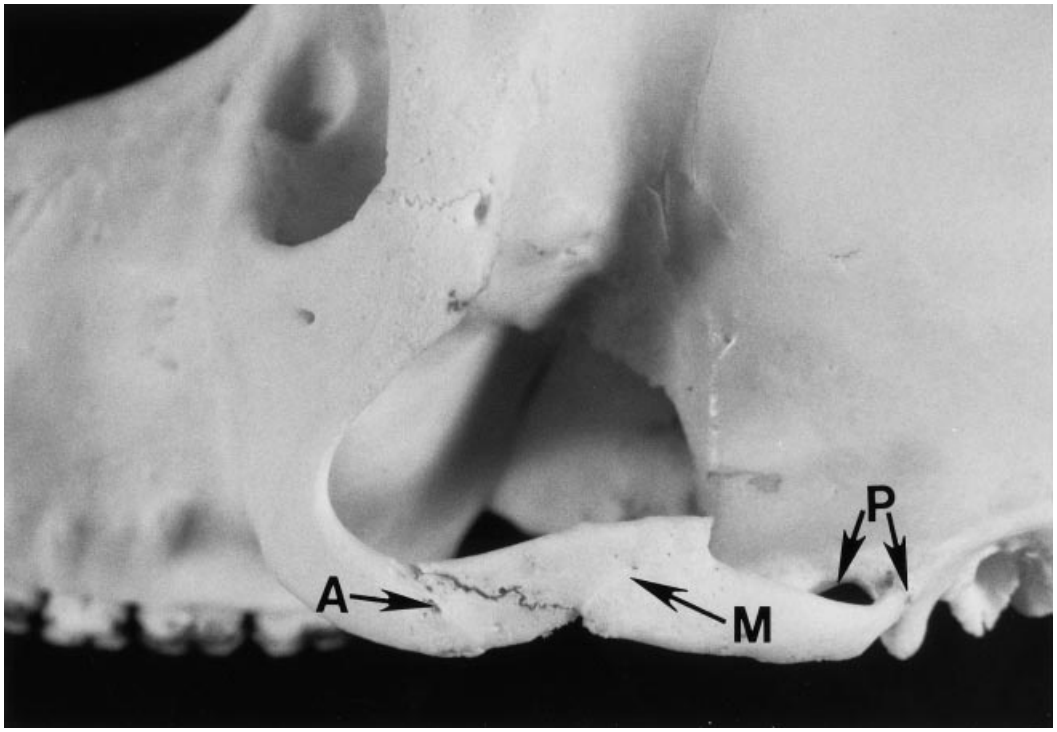

Fig. 10. Photograph of the skull of an adult male Japanese macaque (*Macaca fuscata*) (collection of the Department of Biological Anthropology and Anatomy, Duke University). At some point in the life of this subject the zygomatic arch was fractured into two fragments with three fracture sites. This is a typical fracture pattern for a beam with fixed ends. The anterior (A) and middle (M) fracture sites have healed, although the fragments along the middle site are not properly aligned. Note that the zygomaticotemporal suture is not one of the three fracture sites. The posterior fracture site (P) has resulted in a fibrous union.

for some bones are influenced by the process of "functional adaptation," as suggested by Lanyon and Rubin (1985), then the "optimal strain environment" must indeed vary widely throughout the entire skeleton (cf. Lanyon et al., 1982; Rubin, 1984; Lanyon and Rubin, 1985; Hylander and Johnson, 1992; Biewener, 1993).

Although structural failure of facial bones during chewing and biting is either nonexistent or an extremely rare occurrence, there is considerable evidence for the occurrence of structural failure due to traumatic injuries, and this evidence is not simply limited to data from modern human populations (cf. Schultz, 1939, 1956, 1969; Alexanderson, 1967; Lovell, 1990). Nevertheless, the modern human data are particularly interesting in that they clearly demonstrate, not surprisingly, that when fractured, facial bones are ordinarily loaded quite differently than loads associated with chewing and biting.

The most common structural failures of the human mandible are vertical fractures through the mandibular corpus and symphysis, and oblique fractures through the subcondylar region (Hopkins, 1985). The former usually result from a blow to the side of the jaw and the latter from a blow to the front of the jaw. For the human zygomatic arch, the most common fractures occur when the arch is forcibly driven medially by a blow to the side of the head. When completely fractured, this actually results in three fractures of the arch (Ellis, 1991), which is a typical failure pattern for a beam with fixed ends (Fig. 10). Another common but much more serious type of zygomatic arch fracture is associated with fracture of the entire zygomaxillary complex. This results from a blow to the orbit and anterior root of the zygoma, and this condition involves additional fractures through the postorbital bar and septum, floor of the orbit, and anterior root of the

zygoma. When this occurs there is usually a single fracture through the zygomatic arch, and it is located about 1.5 cm posterior to the zygomatico-temporal suture (Ellis, 1991). In all of these instances, the loading regimes acting on the mandible and zygomatic arch are quite different from the typical predominant regimes that are encountered during chewing and biting (cf. Hylander, 1979c, 1984). This is unlike the situation when long bones fail during normal locomotor behaviors, and perhaps additional instances when long bones fail during accidents where the loading regimes are not too dissimilar to those encountered during locomotion.

The occasional traumatic blow to the face does not invariably result in facial bone fractures, so obviously there are safety factors for facial bones to these sorts of nonmasticatory traumatic loads. If an organism has yet to experience these loads, then obviously the process of "functional adaptation" cannot possibly adjust bone mass so as to provide an appropriate safety factor for these traumatic loads simply because "functional adaptation" cannot respond to loads it has not yet experienced. Of course an increase in bone mass in response to an increase in magnitude of masticatory force will result in a more robust and stronger masticatory apparatus (Bouvier and Hylander, 1981), which in turn will be better able to counter nonmasticatory traumatic loads. This, however, is an inefficient way to increase the safety factor for such traumatic loads because the bone mass will presumably not be optimally distributed for countering traumatic loads if it is in fact adapting solely to masticatory loads. More importantly, modifying safety factors in this manner means that the modification must be linked to modifying chewing and biting behaviors. That is, safety factors for accidental loads must be increased by habitually chewing and biting more forcefully. Instead of altering safety factors only by "functional adaptation," it is more likely that the distribution of bone mass throughout most regions of the cranium is influenced significantly by natural selection on the genetic "blueprint" (Lanyon and Rubin, 1985).

What about the actual size of safety factors in skeletal tissues? It has been suggested by various workers (e.g., Rubin and Lanyon, 1984; Lanyon and Rubin, 1985; Biewener, 1993; Rubin et al., 1994) that as peak functional principal strains in the vertebrate skeleton are in the range of 2,000 to 3,000 με and because cortical bone fails (yields) at about 6,800 με, safety factors for vertebrate bone are for the most part in the range of 2 to 4, e.g., bone strain at failure (6,800 με)/observed peak strain for the macaque zygomatic arch (2,113 με) = 3.2. However, since cortical bone will experience fatigue failure at levels well below 6,800 με (e.g., at about 3,000 με following one million loading cycles; Carter et al., 1977; Carter and Spengler, 1978; Carter, 1984), and since for some mammals behaviors such as mastication (or running, flying, etc.) involve tens of thousands of loading cycles each day (Stobbs and Cowper, 1972), perhaps these safety factor estimates are often simply too high because bone strain levels associated with fatigue failure were not used in their calculation? In addition and very importantly, there are certain areas of the face where the peak functional principal strains are relatively low, i.e., they do not exceed 200 με, and therefore these bony areas have *fatigue* safety factors in excess of 15 and *yield* safety factors in excess of 30 for routine cyclical loads. Furthermore, in those situations involving a single traumatic load, for some bones or areas (such as the rostral interorbital region) it may not matter that it is loaded well beyond the yield point because what is crucial is that the bone tissue remains structurally intact long enough for the yielded area to heal (model and remodel). In these instances, perhaps safety factor estimates should be based on the fact that bone experiences ultimate failure at about 16,000 με, as opposed to monotonic yield failure at 6,800 με, or fatigue failure (following one million loading cycles) at about 3,000 με?

Thus, it would appear that safety factors for vertebrate bones are not restricted to a narrow range of 2 to 4 since the magnitude of functional strains varies considerably and the consequences and types of bone failures must vary appreciably, depending on the species and the involved bone. It could be argued that safety factors in the range of 2 to 4 are confined to load-bearing bones (Lanyon and Rubin, 1985), but then this

raises the issue of how to define a load-bearing bone. This is particularly problematic when dealing with the skull. For example, although the browridge region is strained during chewing and biting, and therefore is load-bearing during these behaviors, its bony architecture is not optimally designed to counter these loads, and its yield safety factor (for masticatory loads) is in excess of 20.

In summary, although it is well recognized that vertebrate bone must have design features that include safety factors related to loads experienced during behaviors such as swimming, flying, running, and chewing (cf. Alexander, 1981), there appears to be less appreciation for safety factors related to nonroutine infrequent traumatic loads (although cf. Lanyon and Rubin, 1985). This may be partly because the concept of safety factors for skeletal structures has been developed primarily by workers interested in the structural failure of long bones (Alexander, 1981), and the failure of long bones occasionally occurs during loading regimes that may not differ greatly from the loads associated with normal locomotion.

In contrast to long bones, traumatic loads to the skull are probably *always* quite different from routine functional loads associated with masticatory forces, and therefore if safety factors for traumatic loads are built into the craniofacial skeleton, these are probably done so by factors other than the process of "functional adaptation." This is simply because this process is unable to anticipate loads it has yet to experience. Moreover, it is also unable to optimize the morphology of the bones so as to minimize the occurrence of these types of fractures if it links modifying safety factors for nonmasticatory traumatic loads solely to modifying masticatory loads.

Presumably the process of "functional adaptation" also does not entirely account for safety factors for many portions of the postcranial skeleton because, for example, long bone fractures frequently occur during accidental falls, and presumably these fractures result from loading regimes that do not closely approximate loads encountered during routine ordinary locomotor behaviors. Thus, surely safety factors have been selected for on the basis of more than simply the loads encountered during routine locomotor behaviors (Alexander, 1981). Finally, presumably a particular bone or bony region in fact has multiple safety factors, depending on whether one considers normal routine cyclical loads, or various single or multiple traumatic loads that are quite unlike the routine cyclical loads of daily life.

Loading of the zygomatic arch

Since during chewing and biting there is a steep strain gradient along the zygomatic arch, a question that immediately arises is why the anterior portion of the arch is strained more than the posterior portion, particularly since the anterior portion has a much denser concentration of bone mass, and therefore must be much stiffer than the posterior portion (see Fig. 8). Furthermore, there is also the question of why the direction of ϵ_1 and the relative size of the ϵ_1/ϵ_2 ratio shifts in such a consistent but reversed manner along working and balancing sides (Tables 4 and 5 and Fig. 7). These questions are importantly related to how the zygomatic arch is loaded.

As the superficial and deep masseter attach directly to the zygomatic arch, during chewing and biting the zygomatic arch must be loaded primarily by the ipsilateral masseter muscle force (cf. Hylander and Johnson, 1989; Herring and Mucci, 1991). An earlier analysis indicates that peak zygomatic arch strains are highly correlated with peak electromyographic (EMG) activity of the superficial masseter, and less so with the much smaller deep masseter (Hylander and Johnson, 1989). Furthermore, as the entire superficial masseter muscle (and a small portion of the deep) attaches along the anterior half of the zygomatic arch, i.e., anterior to the zygomaticotemporal suture (Fig. 2), masseter muscle force must be concentrated anteriorly. This in turn insures that maximum shear force and bending and twisting moments associated with masseter force are also concentrated anteriorly, and this is probably why the largest strains are associated with the anterior portion of the arch. We will return to this issue in a following section that deals with bending and twisting of the zygomatic arch.

Although the superficial masseter has a major influence on strain patterns in the

zygomatic arch, the deep masseter also has an influence on these patterns. In fact, we suspect that the differences in patterns of peak strain between the working and balancing sides are in part due to differential activity between these two portions of the masseter. Furthermore, the changing patterns of zygomatic arch strain throughout the duration of the power stroke are probably also due to these differential patterns. This interpretation is based on the following observations.

Previous analyses have established that in macaques and baboons, peak EMG activity of the working-side deep masseter ordinarily precedes peak activity of the working-side superficial masseter, whereas for the balancing-side masseter, this pattern is reversed or alternated (Hylander and Johnson, 1994). Similarly, there are alternations in the average patterns for the direction of ϵ_1 and for ϵ_1/ϵ_2 values. For example, as seen in Figure 7, for the right zygomatic arch the average direction of ϵ_1 for all three rosette locations shifts in a counterclockwise direction on the working side, and in a clockwise direction on the balancing side. For the left zygomatic arch, these patterns are reversed. Moreover, average values of ϵ_1/ϵ_2 for the working-side arch tend to decrease along the anterior and middle rosettes, and increase along the posterior rosette (Table 4). For the balancing-side arch, the reverse situation prevails. A plausible explanation for the occurrence of the alternating strain patterns along working- and balancing-side zygomatic arches is that they are due to alternating patterns of force from the deep and superficial masseter muscles. Figure 11, which is derived from data of a previous study (Hylander and Johnson, 1994), has been included here to demonstrate differential EMG activity of the superficial and deep portions of the masseter muscle and associated patterns of midzygomatic arch strain. Among other things, this figure demonstrates the late burst of activity of the balancing-side deep masseter and a rather characteristic pattern of balancing-side zygomatic arch strain during unloading that is presumably linked to deep masseter force.

The zygomatic arch strain data also indicate that overall there is more strain along the working side than along the balancing side, and this is likely to be because in primates (and perhaps most other mammals) the working-side masseter usually exerts more force than does the balancing-side masseter during the power stroke (cf. Hylander et al., 1992). Based simply on the grand mean values for maximum shear strain (Table 2), the average working/balancing (W/B) shear strain ratios for the anterior, middle and posterior rosettes when chewing hard/tough foods are 1.1, 1.2, and 1.0, respectively. Comparable values for chewing apple with skin are 1.3, 1.4, and 1.5, respectively. Although these values do not indicate actual average W/B masseter muscle-force ratios because they are derived by dividing average working-side strain values by average balancing-side values, they are quite similar to earlier and more reliable W/B force estimates (Hylander et al., 1992). Furthermore, as the W/B strain ratios for chewing hard/tough food items are smaller than those for chewing less resistant food items, these data are consistent with the hypothesis that the more strenuous power strokes are associated with a disproportionate increase in masseter muscle force from the balancing side (Hylander, 1979b, Crompton and Hylander, 1986; Hylander et al., 1992; Crompton, 1995).

Bending and twisting of the zygomatic arch

Although it is clear that the masseter muscle exerts a major influence on patterns of strain in the zygomatic arch, there still remains the issue of how the zygomatic arch is loaded. This is important for understanding why there is a steep strain gradient along the arch, and it is the main reason for its discussion here. Unfortunately, as our rosettes were confined to restricted locations, our data are incapable of completely resolving this issue, although the following discussion of bending and twisting makes it quite clear why the anterior portion of the arch is strained more than the posterior portion.

Parasagittal bending. When viewed in the lateral projection, it is clear that the vertical component of masseteric force must bend the zygomatic arch in the parasagittal plane. If the zygomatic arch is modeled as a

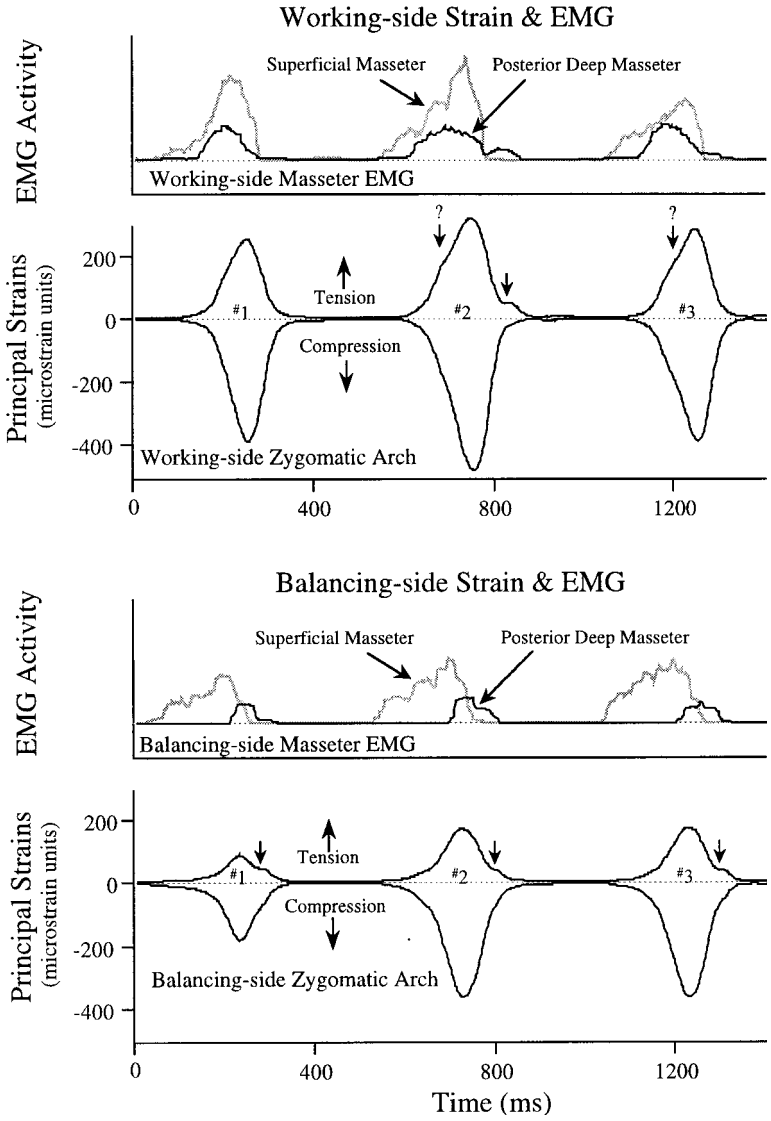

Fig. 11. Simultaneous plots of the principal strains from the middle portion of the zygomatic arch and digitized root-mean-square EMG values of the superficial and deep masseter muscles on both left and right sides. The subject, an adult female *Macaca fascicularis*, is chewing apple skin on the right side. The strain and EMG along the top half of the figure are from the right zygomatic arch and right muscles (i.e., the working side), whereas those along the bottom half are from the left side (i.e., the balancing side). As the physiological cross-sectional area of the superficial masseter is about twice the size of the deep masseter (Antón, 1993), the EMG plots have been scaled so that within these chewing sequence, the largest value for the superficial masseter is double the size of the largest value of the deep masseter. This gives a first-approximation impression of the relative amount of force that each of these muscles is contributing. Note that on the working side the deep masseter peaks prior to the superficial masseter, whereas on the balancing side this pattern is reversed (Hylander and Johnson, 1994). The small unlabeled arrows pointing to the plots of the maximum principal strain (tension) indicate changing strain patterns that are plausibly linked to deep masseter function. These changes are detectable on all three of the balancing-side power stroke strains during unloading (also, see Fig. 10A in Hylander and Johnson, 1994). There is an unusual (but small) secondary burst of the working-side deep masseter during unloading of the #2 power stroke, and as indicated by the small arrow, there is a characteristic pattern of zygomatic arch strain associated with it. Finally, although not readily apparent in this figure, it is common to see a changing pattern of strain during loading along the working side. See small arrows labeled (?) and also Figure 4 in Hylander et al. (1992). Thus, one frequently sees changing patterns of zygomatic arch strains during loading on the working side and during unloading on the balancing side, and these changes appear to be associated with distinctive activity patterns of the deep masseter relative to the superficial masseter.

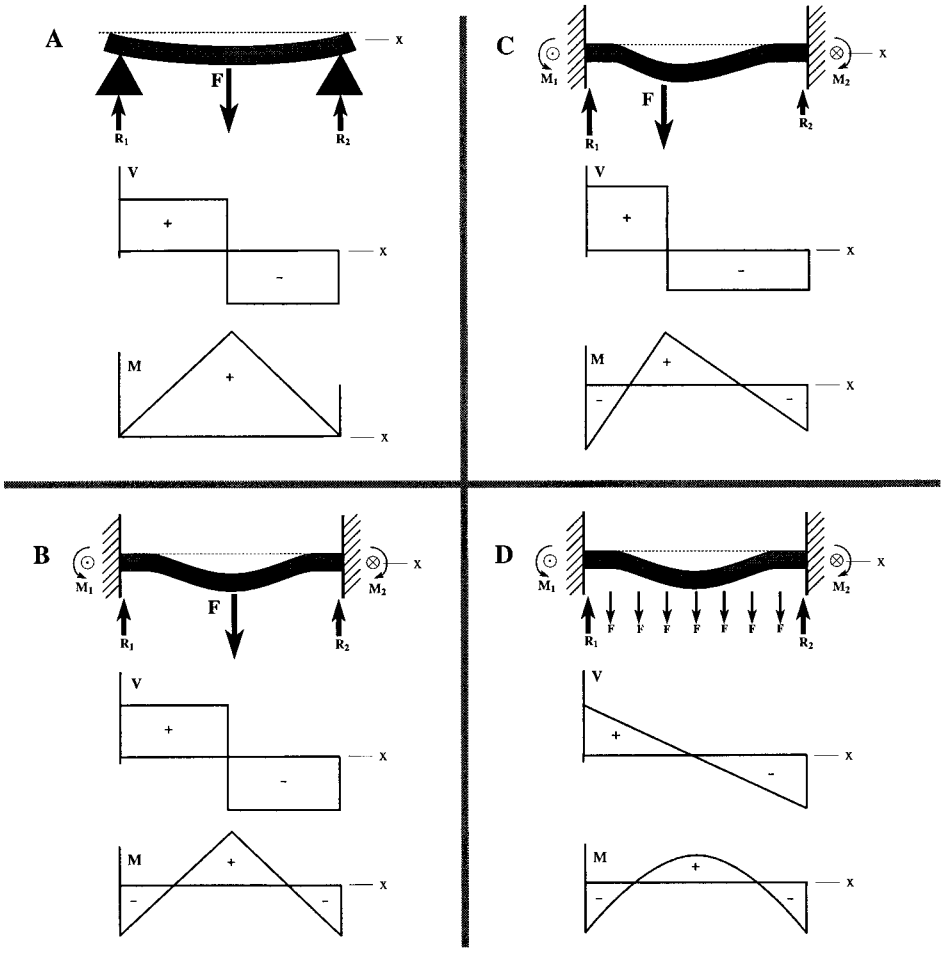

Fig. 12. Deflection patterns and moment diagrams. F, R, V, and M indicate applied force, reaction force, shear force, and bending moments, respectively. M_1 and M_2 indicate internal moments associated with the ends of fixed beams. $R_1 + R_2 = F$. **A:** A supported but unfixed beam with a center load F. Note that the largest moment is located along the center of the beam and the moments are zero at the ends. The shear force (V) is equal and opposite to the left and right of F. **B:** A beam fixed at both ends with a center load F. Note that the largest moment is located along the center of the beam, although it is less than the moment in A. Note also that the moments along the ends of the beam are not zero and they are reversed in direction due to the internal moments (M_1 and M_2) associated with fixed beams. The shear force is distributed as in A. **C:** A beam fixed at both ends and an off-center load F. Note again that the moments are reversed along the ends. Furthermore, note that the largest moment is along the left end of the beam, which is the end closest to the load F. The largest shear force is also along the left side. **D:** A beam fixed at both ends with a uniform load equal to F, i.e., 7F = F. (The F in D, although smaller in the figure, is equal to F in A, B, and C.) Note again that the moments are reversed along the ends of the beam. Moreover, the bending moments and shear force along the ends are larger than those along the center. In fact, shear force is near zero along the center. This figure is adapted from Shigley and Mitchell (1983).

beam with unfixed but supported ends and loaded by a vertical force along the middle of the beam, the deflection pattern of such a beam is indicated in Figure 12A. Modeling the zygomatic arch in this manner, however, is inappropriate because the zygomatic arch is fixed (or restrained) at both ends. The deflection pattern of a beam that is fixed at both ends is indicated in Figures 12B, C, and D. Note in Figure 12B that although much of the lower border of the beam must experience tensile stress as its upper border experiences compressive stress, there is a reversed pattern of bending stress (and moments) near its two ends. Near the ends the lower border of the beam experiences

compressive stress, whereas its upper border experiences tensile stress. Note in Figure 12C that when the beam experiences an off-center load by shifting F to the left, the largest bending moments are not necessarily located at that point where the applied force intersects the beam. In this instance the largest bending moment is at the very end of the beam, closest to the applied force. If the left end of the beam is considered to be towards the anterior portion of the arch, this figure more accurately simulates the position of the resultant force of the masseter, and also indicates that the largest bending moments are towards the anterior portion of the arch. Note also that shearing forces are also larger "anteriorly."

Figure 12D indicates a fixed beam that is uniformly loaded, rather than loaded at a point location. In this figure, shearing forces and bending moments at the ends of the beam are larger than those in the middle. Force distribution of the masseter for parasagittal bending is probably best modeled as some combination of the condition seen in Figures 12C and 12D, i.e., loaded throughout its extent but with most of the force concentrated along the more anterior portion of the arch. Under these conditions the largest bending moments and shearing forces are located along the most anterior portion of the arch, and the bone strain data indicate that this is the region that experiences the most strain.

Modeling the zygomatic arch as a homogeneous beam with fixed ends and loaded in some combination of external forces as indicated in Figures 12C and 12D, however, is an oversimplification. This is not only because facial bone is anisotropic (Dechow et al., 1993), but also because there is a suture present within the middle of the zygomatic arch, the zygomaticotemporal suture (Fig. 2). Since ontogenetically the zygomaticotemporal suture tends to become increasing more rigid and eventually ossifies (Bouvier and Hylander, 1996a), the inability to model the biomechanical properties of this suture may be a particularly significant problem when dealing with immature subjects. An analysis of the zygomatic arch is further complicated because the temporalis fascia, which is thought to provide a suspensory bracing for the zygomatic arch (Sicher, 1950; Weinman and Sicher, 1955; Eisenberg and Brodie, 1965), is very difficult to model biomechanically. Parenthetically, additional evidence to support the suspensory bracing hypothesis comes from observations indicating that when the human zygomatic arch is fractured into several fragments, the masseter does not displace these fragments inferiorly (Alling, 1988; and Fig. 10).

As the three rosettes in this study were located midway between the upper and lower borders of the zygomatic arch (Fig. 2), the patterns of recorded strain cannot provide an unambiguous test of the parasagittal bending hypothesis. This is because these rosettes are not in position to record strain primarily from near the upper and lower borders of the zygomatic arch so as to confirm possible simultaneous tensile and compressive bending strains. The direction of the principal strains for the anterior and posterior rosette locations are, however, consistent with expected patterns of shear strain along the neutral axis during parasagittal bending. The strain directions of the middle rosette, however, are not consistent with these patterns.

In summary, although the data from this study are unable to resolve the relative importance of parasagittal bending, based on the anatomical configuration of the zygomatic arch and masseter muscle, the zygomatic arch is likely bent in the parasagittal plane, with the largest bending moments and shearing forces presumably concentrated along the anterior portion of the arch.

Transverse bending. When the macaque zygomatic arch is viewed from above, the medially directed component of force from the masseter muscle must bend the zygomatic arch in the transverse plane. That is, the zygomatic arch is pulled medially towards the neurocranium. This type of bending causes the middle segment of the lateral aspect of the arch to experience compressive stress, whereas its medial aspect experiences tensile stress. Moreover, as the ends of the zygomatic arch are fixed, these patterns of bending stress are reversed along its anterior and posterior ends (see Fig. 12B).

Similar to the situation for parasagittal bending, the patterns of recorded strain

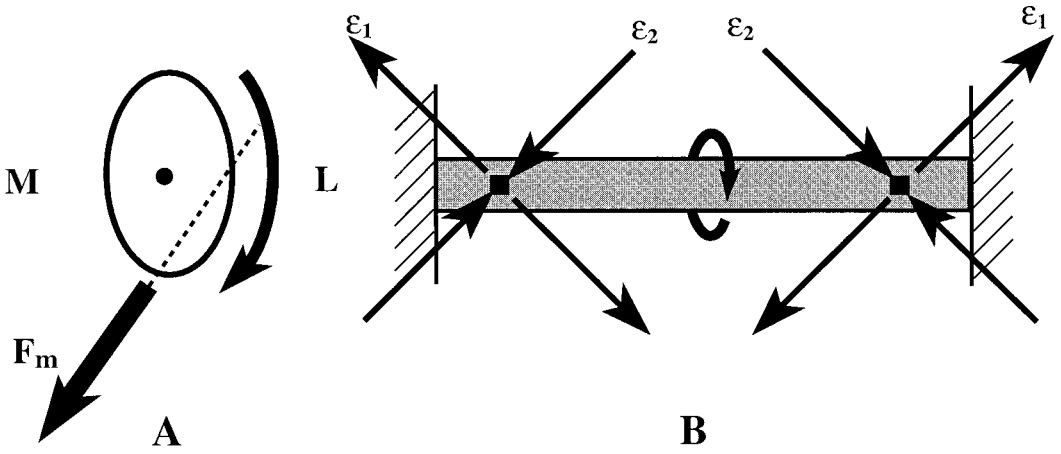

Fig. 13. Twisting an oval uniform bar that is fixed at both ends. **A:** A drawing of a cross-section of a hypothetical zygomatic arch. M and L indicate medial and lateral surfaces, respectively. The large straight arrow labeled F_m indicates the direction of pull of the entire masseter muscle. F_m twists the zygomatic arch about its long axis. This twisting tends to invert the lower border of the arch and evert its upper border. The black dot indicates the approximate location of the twisting axis of neutrality. The large curved arrow indicates the direction of twisting. **B:** The fixed bar is twisted as indicated by the curved arrow. The direction of the principal strains along the solid squares located at the two ends of the bar are indicated by the labeled arrows; ϵ_1 = principal tension and ϵ_2 = principal compression. If the force associated with the twisting moment is located in the middle of the bar (see curved arrow), strains along the ends are identical in magnitude (but opposite in direction). If the force is shifted to the left, strains along the left side increase whereas those along the right side decrease.

from the three rosettes along the lateral aspect of the zygomatic arch cannot provide an unambiguous test of the transverse bending hypothesis. Strain recordings from the medial aspect of the arch would have been very helpful towards this end, but this was impossible to accomplish without extensive and undesirable surgical alterations on the temporalis fascia. Nevertheless, data from the middle rosette are more or less compatible with the transverse bending hypothesis in that principal compression (ϵ_2) is aligned near parallel to the long axis of the arch (Figs. 5 and 6) and ϵ_2 is much larger than principal tension (ϵ_1; Table 4). Data from the anterior and posterior rosettes, however, do not provide support for the transverse bending hypothesis because the principal strains along these areas tend to be aligned close to 45 degrees relative to the long axis of the arch.

Twisting. As most of the masseter muscle attaches along the lower border of the zygomatic arch and because the masseter muscle has a medially directed component of force, there is a tendency for the zygomatic arch to be also twisted about its long axis (Fig. 13A). This twisting or torsion causes the lower border of the arch to invert and its upper border to evert.

If the zygomatic arch is twisted in the above-described manner, ϵ_1 along its ends would be aligned at 45 degrees relative to the long axis of the arch (as indicated in Fig. 13B). Moreover, ϵ_1/ϵ_2 would be near equal to 1.0. As ϵ_1 is directed upwards and forwards near 45 degrees along the anterior rosette and upwards and backwards at near 45 degrees along the posterior rosette and as the values of ϵ_1/ϵ_2 for these two rosette locations are near equal to 1.0, these data tend to support the twisting hypothesis (Figs. 5 and 6 and Table 4). Furthermore, since both ends of the arch are fixed and because the masseter muscle force is concentrated more anteriorly, the largest twisting moments and strain magnitudes should be located along the anterior portion of the arch. As noted previously, the largest strains are indeed found along the anterior portion. Nevertheless, these same observations on strain directions also support the presence of parasagittal bending, and therefore we are unable at this time to determine the relative importance of these various bending and twisting regimes.

Summary of zygomatic arch loads. Based solely on anatomical considerations, it is likely that the zygomatic arch is simultaneously bent in both the parasagittal and transverse planes and twisted about its long axis. Unfortunately, anatomical constraints influencing rosette position do not allow us to rigorously test these hypotheses, i.e., allow us to evaluate the relative contributions of these loading regimes. Perhaps the best way to resolve the issue as to how the zygomatic arch is loaded is to do a detailed finite-element analysis of the arch, and to then use the in vivo strain data for validation purposes. Work currently in progress is investigating this possibility (Borrazzo et al., 1994), and preliminary results suggest that during mastication, the zygomatic arch is primarily twisted about its long axis by an anteriorly located moment. On the other hand, if morphology of the highly strained anterior portion of the macaque zygomatic arch is a reflection of the relative importance of the above bending and twisting loads, it appears that parasagittal bending is of considerable importance (as it is for the mandibular corpus) because a cross-section of the anterior portion of the macaque zygomatic arch (Fig. 8) is near oval with its major axis aligned dorsoventrally (cf. Hylander 1979a,c). Finally, although the relative contributions of the above bending and twisting regimes are unclear, all of these regimes (particularly parasagittal bending and twisting) result in larger shearing forces and moments, and therefore larger strains, along the anterior portion of the zygomatic arch.

CONCLUSIONS

An analysis of in vivo bone strain throughout the face of macaques indicates the clear absence of a high and near uniform strain environment. These data indicate that as levels of functional strains during chewing and biting are highly variable from one region of the face to the next, it is unlikely that all facial bones are especially designed so as to minimize bone tissue and maximize strength for countering masticatory loads. Thus, the functional significance of the morphology of certain facial bones need not necessarily bear any important or special relationship to routine and habitual cyclical mechanical loads associated with chewing or biting. Furthermore, the presence of these steep strain gradients within the facial skeleton suggests that the amount of bone mass in the low-strain areas may be largely determined by factors unrelated to processes frequently referred to as "functional adaptation," or conversely, that the "optimal strain environment" of bone varies enormously throughout the facial skeleton. Nevertheless, it is quite clear that functional strains have an important influence on the development and maintenance of certain facial bones, such as the mandible (Bouvier and Hylander, 1981). On the other hand, a significant but undefined portion of the anatomy of the facial skeleton of primates is due to more than simply the countering and dissipating of masticatory force.

ACKNOWLEDGMENTS

This study was supported by the Department of Biological Anthropology and Anatomy, Duke University. We thank Dr. Farsh Guilak for his assistance on the mechanics of fixed beams, and Drs. Callum Ross, Matt Ravosa, Marianne Bouvier, Christine Wall, and Daniel Schmitt for helpful comments on an earlier draft of this manuscript. We also thank the three anonymous reviewers for their many helpful and insightful comments.

LITERATURE CITED

Alexander RM (1981) Factors of safety in the structure of animals. Sci. Prog. *67:*109–130.

Alexandersen V (1967) The evidence for injuries to the jaws. In D Brothwell and AT Sandison (eds.): Diseases in Antiquity. Chap. 49. Springfield, IL: Thomas, pp. 1–7.

Alling CCI (1988) Fractures at the zygomatic arch and the zygomaticomaxillary complex. In CCI Alling and DB Osbon (eds.): Maxillofacial Trauma. Philadelphia: Lea & Febiger, pp. 333–362.

Antón SC (1993) Internal masticatory muscle architecture in the Japanese macaque and its influence on bony morphology. Am. J. Phys. Anthropol. Suppl. *16:*50.

Bassett CAL (1968) Biological significance of piezoelectricity. Calcif. Tissue Res. *1:*252–272.

Biewener AA (1990) Biomechanics of mammalian terrestrial locomotion. Science *250:*1097–1103.

Biewener AA (1993) Safety factors in bone strength. Calcif. Tissue Int. *53*(Suppl 1):S68–S74.

Biknevicius AR, and Ruff CB (1992) The structure of the mandibular corpus and its relationship to feeding behaviours in extant carnivorans. J. Zool. Lond. *228:* 479–507.

Borrazzo EC, Hylander WL, and Rubin CT (1994) Validation of a finite element model of the functionally

loaded zygomatic arch by in vivo strain gage data. Proc. Am. Soc. Biomech. *18:*51–52.

Bouvier M, and Hylander WL (1981) Effect of bone strain on cortical bone structure in macaques (*Macaca mulatta*). J. Morphol. *167:*1–12.

Bouvier M, and Hylander WL (1994) Bone remodeling responses to strain gradients in the zygomatic arch of macaques. J. Dent. Res. *73:*195.

Bouvier M, and Hylander WL (1997) The functional of secondary osteonal bone: Mechanical or metabolic? Arch. Oral Biol. (in press).

Bouvier M, and Hylander WL (1997) Strain gradients, age, and levels of modeling and remodeling in the facial bones of *Macaca fascicularis*. In, Z. Davidovitch and L.A. Norton (eds.): The Biological Mechanisms of Tooth Movement and Craniofacial Adaptation. Birmingham, AL: EBSCO Media. Harvard Society for the Advancement of Orthodontics, pp. 407–412.

Carter DR (1984) Mechanical loading histories and cortical bone remodeling. Calcif. Tissue Int. *36:*S19–S24.

Carter DR (1987) Mechanical loading history and skeletal biology. J. Biomech. *20:*1095–1109.

Carter DR, and Spengler DM (1978) Mechanical properties and composition of cortical bone. Clin. Orthop. *135:*192–217.

Carter DR, Spengler DM, and Frankel VH (1977) Bone fatigue in uniaxial loading at physiologic strain rates. IRCS J. Med. Sci. *5:*592.

Connolly R, and Quimby FW (1978) Acepromazine-ketamine anesthesia in the rhesus monkey (*Macaca mulatta*). Lab. Anim. Sci. *28:*72–74.

Crompton AW (1995) Masticatory function in nonmammalian cynodonts and early mammals. In JJ Thomason (ed.): Functional Morphology in Vertebrate Paleontology. Cambridge: Cambridge Univ. Press, pp. 55–75.

Crompton AW, and Hylander WL (1986) Changes in mandibular function following the acquisition of the dentary-squamosal jaw articulation. In N Hotton, PD MacLean, and JJ Roth (eds.): The Ecology and Biology of Mammal-like Reptiles. Washington, D.C.: Smithsonian Institution Press, pp. 263–282.

Currey J (1984) The Mechanical Adaptations of Bones. Princeton, NJ: Princeton University Press.

Daegling DJ (1993) The relationship of *in vivo* bone strain to mandibular corpus morphology in *Macaca fascicularis*. J. Hum. Evol. *25:*247–269.

Dechow PC, Nail GA, Schwartz-Dabney CL, and Ashman RB (1993) Elastic properties of human supraorbital and mandibular bone. Am. J. Phys. Anthropol. *90:*291–306.

Demes B (1987) Another look at an old face: Biomechanics of the neandertal facial skeleton reconsidered. J. Hum. Evol. *16:*297–303.

DuBrul EL (1988) Sicher and DuBrul's Oral Anatomy. St. Louis: Ishiyaku EuroAmerica.

Eisenberg NA, and Brodie AG (1965) Antagonism of temporal fascia to massetric contraction. Anat. Rec. *152:*185–192.

Ellis EI (1991) Fractures of the zygomatic complex and arch. In RJ Fonseca and RV Walker (eds.): Oral and Maxillofacial Trauma. Philadelphia: W.B. Saunders, pp. 435–514.

Frost HM (1986) Intermediary Organization of the Skeleton. Boca Raton: CRC Press.

Goodship AE, Lanyon LE, and McFie H (1979) Functional adaptation of bone to increased stress. J. Bone Jt. Surg. *61A:*539–546.

Greaves WS (1985) The mammalian postorbital bar as a torsion-resisting helical strut. J. Zool. Lond. *207:*125–136.

Herring SW, and Mucci RJ (1991) In vivo strain in cranial sutures: The zygomatic arch. J. Morphol. *207:*225–239.

Hopkins R (1985) Mandibular fractures: treatment by closed reduction and indirect skeletal fixation. In NL Rowe and JL Williams (eds.): Maxillofacial Injuries. Edinburgh: Churchill Livingstone, pp. 232–292.

Hylander WL (1979a) The functional significance of primate mandibular form. J. Morphol. *160:*223–240.

Hylander WL (1979b) An experimental analysis of temporomandibular joint reaction force in macaques. Am. J. Phys. Anthropol. *51:*433–456.

Hylander WL (1979c) Mandibular function in *Galago crassicaudatus* and *Macaca fascicularis:* An *in vivo* approach to stress analysis of the mandible. J. Morphol. *159:*253–296.

Hylander WL (1984) Stress and strain in the mandibular symphysis of primates: A test of competing hypotheses. Am. J. Phys. Anthropol. *64:*1–46.

Hylander WL (1985) Mandibular function and biomechanical stress and scaling. Am. Zool. *25:*315–330.

Hylander WL (1986) *In vivo* bone strain as an indicator of masticatory bite force in *Macaca fascicularis*. Arch. Oral Biol. *31:*149–157.

Hylander WL, and Johnson KR (1989) The relationship between masseter force and masseter electromyogram during mastication in the monkey *Macaca fascicularis*. Arch. Oral Biol. *34:*713–722.

Hylander WL, and Johnson KR (1992) Strain gradients in the craniofacial region of primates. In Z Davidovitch (ed.): The Biological Mechanisms of Tooth Movement and Craniofacial Adaptation. Columbus, Ohio, U.S.A.: Ohio State University College of Dentistry, pp. 559–569.

Hylander WL, and Johnson KR (1994) Jaw muscle function and wishboning of the mandible during mastication in macaques and baboons. Am. J. Phys. Anthropol. *94:*523–547.

Hylander WL, and Ravosa MJ (1992) An analysis of the supraorbital region of primates: A morphometric and experimental approach. In P Smith and E Tchernov (eds.): Structure, Function and Evolution of Teeth. London: Freund, pp. 223–255.

Hylander WL, Picq PG, and Johnson KR (1987) A preliminary stress analysis of the circumorbital region in *Macaca fascicularis*. Am. J. Phys. Anthropol. *72:*214.

Hylander WL, Picq PG, and Johnson KR (1991) Masticatory-stress hypotheses and the supraorbital region of primates. Am. J. Phys. Anthropol. *86:*1–36.

Hylander WL, Johnson KR, and Crompton AW (1992) Muscle force recruitment and biomechanical modeling: An analysis of masseter muscle function in *Macaca fascicularis*. Am. J. Phys. Anthropol. *88:*365–387.

Kimmel DB (1993) A paradigm for skeletal strength homeostasis. J. Bone Mineral Res. *8*(Suppl. 2):S515–S522.

Koch JC (1917) The laws of bone architecture. J. Anat. *21:*177–298.

Kummer BKF (1972) Biomechanics of bone: Mechanical properties, functional structure, functional adaptation. In: YC Fung, N Perrone, and M Anliker (eds): Biomechanics: Its Foundations and Objectives. Englewood Cliffs: Prentice Hall Inc; pp. 237–271.

Lanyon LE (1973) Analysis of surface bone strain in the calcaneus of sheep during normal locomotion. J. Biomech. *6:*41–49.

Lanyon LE (1991) Biomechanical properties of bone and response of bone to mechanical stimuli: Functional strain as a controlling influence on bone modeling and remodeling behavior. In BK Hall (ed.): Bone Matrix and Bone Specific Products. Ann Arbor, Michigan: CRC Press, pp. 79–108.

Lanyon LE, and Rubin CT (1985) Functional adaptation in skeletal structures. In M Hildebrand, DM Bramble, KF Liem, and DB Wake (eds.): Functional Vertebrate Morphology. Cambridge: Harvard University Press, pp. 1–25.

Lanyon LE, Goodship AE, Pye CJ, and MacFie JH (1982) Mechanically adaptive bone remodelling. J. Biomech. *15:*141–154.

Liskova M, and Hert J (1971) Reaction of bone to mechanical stimuli. Part 2. Periosteal and endosteal reaction of tibial diaphysis in rabbit to intermittent loading. Folia morph., Prague *19:*301–317.

Lovell NC (1990) Patterns of Injury and Illness in Great Apes. Washington: Smithsonian Institution Press.

Martin RB, and Burr DB (1989) Structure, Function, and Adaptation of Compact Bone. New York: Raven Press.

Morey ER, and Baylink DJ (1978) Inhibition of bone formation during space flight. Science *201:*1134–1141.

Morrison NA, Qi JC, Tokita A, Kelly PJ, Crofts L, Nguyen TV, Sambrook PN, and Eisman JA. (1994) Prediction of bone density from vitamin D receptor alleles. Nature *367:*284–287.

Moss ML, and Young RW (1960) A functional approach to craniology. Am. J. Phys. Anthropol. *18:*281–292.

Murray PDF (1936) Bones. A study in the Development and Structure of the Vertebrate Skeleton. Cambridge: Cambridge University.

Nunamaker DM, Butterweck DM, and Provost MT (1990) Fatigue fractures in thoroughbred racehorses: Relationships with age, peak bone strain, and training. J. Orthop. Res. *8:*604–611.

Oyen OJ, Rice RW, and Cannon MS (1979) Browridge structure and function of Neanderthals and extant primates. Am. J. Phys. Anthropol. *51:*83–96.

Pauwels F (1980) Biomechanics of the Locomotor Apparatus. Berlin, Heidelberg, New York: Springer-Verlag.

Preuschoft H, Demes B, Meyer M, and Bär HF (1986) The biomechanical principles realised in the upper jaw of long-snouted primates. In JG Else and PC Lee (eds.): Primate Evolution. Cambridge: Cambridge University Press, pp. 249–264.

Rak Y (1983) The Australopithecine Face. New York, Academic Press.

Rak Y (1986) The Neanderthal: A new look at an old face. J. Hum. Evol. *15:*151–164.

Ravosa MJ (1988) Browridge development in Cercopithecidae: A test of two models. Am. J. Phys. Anthropol. *76:*535–555.

Ravosa MJ (1991) Interspecific perspective on mechanical and nonmechanical models of primate circumorbital morphology. Am. J. Phys. Anthropol. *86:*369–396.

Roberts WE, Garetto LP, and Katona TR (1992) Principles of orthodontic biomechanics: Metabolic and mechanical control mechanisms. In DS Carlson and SA Goldstein (eds.): Bone Biodynamics in Orthodontic and Orthopedic Treatment. Ann Arbor, Michigan: University of Michigan, pp. 189–255.

Roux W (1881) Der züchtende Kampf der Teile, oder die 'Teilauslese' im Organismus. (Theorie der 'funktionellen Anpassung'). Leipzig: Wilhelm Engelmann.

Rubin CT (1984) Skeletal strain and the functional significance of bone architecture. Calcif. Tissue Int. *36:*S11–S18.

Rubin CT, and Lanyon LE (1984) Dynamic strain similarity in vertebrates: An alternative to allometric limb bone scaling. J. Theor. Biol. *107:*321–327.

Rubin CT, Gross TS, Donahue HJ, Guilak F, and McLeod KJ (1994) Physical and environmental influences on bone formation. In C Brighton, G Friedlander and J Lane (eds.): Bone Formation and Repair. Am. Acad. of Orthop. Surg., pp. 61–78.

Russell MD (1985) The supraorbital torus: "A most remarkable peculiarity". Curr. Anthropol. *26:*337–360.

Schultz AH (1939) Notes of diseases and healed fractures of wild apes. Bull. Hist. Med. *7:*571–582.

Schultz AH (1956) The occurrence and frequency of pathological and teratological conditions and of twinning among nonhuman primates. Primatologia *1:*965–1014.

Schultz AH (1969) The Life of Primates. New York: Universe Books.

Scott JH (1967) Dento-facial Development and Growth. New York: Pergamon.

Seipel CM (1948) Trajectories of the jaws. Acta Odonto. Scandinav. *8:*81–191.

Shigley JE, and Mitchell LD (1983) Mechanical Engineering Design. New York: McGraw-Hill.

Sicher H (1950) Oral Anatomy. St. Louis: C.V. Mosby.

Slemeda CW, Christian JC, Williams CJ, Norton JA, and Johnston CC Jr (1991) Genetic determinants of bone mass in adult women: A reevaluation of the Twin Model and the potential importance of gene interaction on heritability estimates. J. Bone Mineral Res. *6:*561–567.

Stobbs TH, and Cowper LJ (1972) Automatic measurement of the jaw movements of dairy cows during grazing and rumination. Tropical Grasslands *6:*107–112.

Tappen NC (1978) The vermiculate surface pattern of brow ridges in Neandertal and modern crania. Am. J. Phys. Anthropol. *49:*1–10.

Ward SC (1991) Taxonomy, paleobiology, and adaptations of the "robust" australopithecines. J. Hum. Evol. *21:*469–483.

Weinmann JP, and Sicher H (1955) Bone and Bones. St. Louis: C.V. Mosby Co.

Wolpoff MH (1980) Paleoanthropology. New York: Knopf.